

Predicting bottom current deposition and erosion on the ocean floor

Daan Beelen^{1,2}  | Lesli J. Wood²

¹Department of Physical Geography, Utrecht University, Utrecht, the Netherlands

²Department of Geology and Geological Engineering, Colorado School of Mines, Golden, Colorado, USA

Correspondence

Daan Beelen, Department of Physical Geography, Utrecht University, Princetonlaan, Utrecht, the Netherlands.

Email: d.beelen@uu.nl; dbeelen@mines.edu

Funding information

SAnD Consortium

Abstract

Mapping sediment deposition and erosion by thermohaline ocean bottom currents is important for the development of ocean infrastructure, future geo resources and understanding the sedimentology of contourites and abyssal sediment wavefields. However, only a limited percentage (estimated 20%) of the ocean floor has been mapped directly through seismic or sonar imaging. To better delineate where zones of bottom current deposition and erosion exist, we develop a prediction from numerical model solutions and sedimentological measurements of the ocean floor. This is achieved by integrating three types of data, which include the following: (1) bottom current shear stress from a model run of the HYCOM numerical ocean model; (2) sedimentation rates from ocean lithospheric age and sediment thickness from the GlobSed Model; (3) the measured extents of bottom current deposits from sonar observations. Shear stresses and sedimentation rates inside and outside the mapped extents of bottom current deposits allow us to quantify the conditions that are conducive for bottom current deposition. These conditions are then extrapolated and displayed on a 1/12° arcsecond resolution map of the world's oceans and validated through comparison with known, mapped systems. Based on our prediction, around 12% of the ocean has significant deposition by bottom currents while only 1% has erosion. Most bottom current activity occurs where thermohaline currents impinge upon the ocean floor like on continental slopes or some areas of the abyssal plain. Deposition and erosion also occur where constriction of ocean bottom currents takes place as in straits and seaways. Inland basins (i.e. seas) and continental shelves are mostly disconnected from global-ocean thermohaline bottom current conveyors and, therefore, have limited bottom current deposition and erosion. Mid-ocean ridges also have little bottom current deposition due to low sediment supply.

KEYWORDS

bottom current, contourite, deposition and erosion on the ocean floor, machine learning, sedimentology

This is an open access article under the terms of the [Creative Commons Attribution-NonCommercial](https://creativecommons.org/licenses/by-nc/4.0/) License, which permits use, distribution and reproduction in any medium, provided the original work is properly cited and is not used for commercial purposes.

© 2023 The Authors. *Basin Research* published by International Association of Sedimentologists and European Association of Geoscientists and Engineers and John Wiley & Sons Ltd.

1 | BACKGROUND

1.1 | Deep ocean processes

The deep marine realm remains the largest and least understood depositional environment on Earth, in spite of the fact that the ocean floor experiences a limited range of erosional and depositional processes. These processes are dominantly driven by thermohaline circulation; a continuous overturning of vast water masses, driven by several ‘deepwater formation pumps’ located near the Earth’s poles (Bullister et al., 2013). Zones of deepwater formation generate relatively dense water through cooling and salinification of ocean surface waters. In these areas of deepwater formation, surface waters sink to the ocean bottom and then emanate across the entire ocean floor, driving a global conveyor of deep ocean currents. Bottom water masses eventually reach areas of upwelling, which are typically adjacent to steep, active continental margins (Xie & Hsieh, 1995). Coastal upwelling brings deep ocean waters back to the surface through a complex series of mostly wind-driven processes, notably Ekman transport (Jacox et al., 2018; Xie & Hsieh, 1995). In between deepwater formation and coastal upwelling, the speed and direction of bottom currents are largely controlled by the topography of the seafloor and the location of Earth’s continents (Rebesco et al., 2014). Furthermore, the rotation of the Earth leads to a so-called ‘geostrophic’ deflection of bottom currents through the Coriolis Effect. These factors combine to form a continuous pattern of deepwater currents called geostrophic bottom currents, or simply, bottom currents. Most bottom currents on the abyssal plain are decoupled from shallow and middle water masses through kinetic barriers that are defined by rapid temperature, pressure and salinity changes in the oceanic water column. One such barrier is the thermocline; a well-defined layer of uniquely sharp changes in temperature that typically sits 400–1000 m below the ocean surface (Zenk, 2008). The thermocline, similar in nature to oceanographic barriers like the salt-content controlled halocline, separates the ocean into stratified volumes called surface, intermediate, deep and bottom waters (Cheng et al., 2020; Stow et al., 2018). Each of these ocean volumes has a unique regime of currents that act on sediments, but the currents that impinge most dominantly on oceanic sediments are bottom currents. Aside from thermohaline circulation, deep tides and abyssal storms are also important processes that move sediments on the ocean floor, but the relative importance of thermohaline currents with respect to tidal processes and other processes in deep ocean environments remains not fully resolved and is an ongoing research pursuit (Hüneke & Stow, 2008; Rebesco et al., 2014; Stow et al., 2018).

Highlights

- Bottom shear stress and sediment availability control the distribution of contourites and abyssal sediment wavefields.
- A global model for bottom currents shows the distribution of depositional and erosional zones.
- Areas that commonly have bottom current deposition are: continental slopes, platforms and other obstructions on the ocean floor.
- Areas that commonly have bottom current erosion are: sea straits and continental slopes affected by strong boundary currents.
- Areas that commonly have bottom current stasis (neither deposition nor erosion) are: mid-ocean ridges and enclosed basins like Mediterranean Seas.

Bottom currents tend to be relatively slow (typically 0.01–0.5 m/s; Hollister & Heezen, 1972; Stow et al., 2009), yet omnipresent and incessant. They shape the geomorphology of vast portions of the ocean floor by entraining, transporting and depositing material on the continental slope and the abyssal plain (Heezen, 1959; Hernández-Molina et al., 2009; Rebesco et al., 2014). Bottom currents do fluctuate in intensity, but overall, the deep marine realm is relatively predictable and less stochastic than the continental or shallow marine realms, on average having less rapid fluctuations in current intensities. This stability allows for accurate numerical modelling of the direction and intensity of shear stresses that act on the ocean floor (Chassignet et al., 2009; Thran et al., 2018). Arguably, ocean bottom currents are one of the most important processes in sedimentology, as they dominate the largest depositional environment on Earth (the abyssal plain), have the longest continuous effects (typically longer than several million years) and generate the largest bedforms on Earth (Flood et al., 1993). Despite this, deposits that have been formed by bottom processes are likely the most poorly understood of deposits because they are hard to reach for study and because ancient bottom current deposits identified on land (surface outcrop analogues) are rare, due to their low preservation potential on geological timescales, a function of continuous recycling and subduction of the oceanic lithosphere (Beelen, 2021; Hüneke & Stow, 2008; Rebesco et al., 2014; Stow et al., 1998).

1.2 | Deep ocean sedimentation

Sediment supply in oceanic regions is supplied through (1) detrital sediment derived from continents, which is

then transferred to the ocean floor through sediment gravity flows and bottom currents, and (2) fallout of water-column suspended sediments. The relative fraction of these sources remains an open question (Beelen, 2021; Velde, 2013). The first component (1) is mostly comprised of gravity-induced processes like turbidity currents, which move eroded material from terrestrial or shallow marine regions into the deep ocean. Turbidity currents can propagate for thousands of kilometres away from their source areas, across the abyssal plain and thereby supply the deepest reaches of ocean basins with sediments (Weaver & Kuijpers, 1983). The second important source for oceanic sediment (2), is mostly biogenic material (biogenic silica and calcium carbonate; Bankole et al., 2020) produced as skeletal tissue of perished planktonic marine organisms settles (falls out) of the water column. Carbonaceous authigenic sediments, which are dominant in some areas of ocean (Stow et al., 2008), also experience dissolution which prevents accumulation of such sediments below the carbonate compensation depth (Stow et al., 2008). Windblown sediment that lands in the ocean eventually settles onto the ocean floor, thereby also contributing to deep ocean sedimentation. Finally, cosmogenic sedimentation from outer space (tektites and [micro] meteorites) also contributes a minor amount (<1 mass percent according to Bankole et al. [2020]).

1.3 | Nomenclature

A common term in the field of deepwater sedimentology is 'contourite', which is a sedimentary deposit formed by bottom currents in deep oceans and seas. The term 'contourite' is synonymous with 'contourite drift' and was initially defined as 'a sedimentary deposit in the deep sea that is formed by (bathymetric) contour-parallel thermohaline currents' (Heezen & Hollister, 1972) and later as 'a sediment accumulation driven by bottom currents, that trend the contours of ocean bathymetry maps' (Stow & Lovell, 1979). The slope-parallel character of these deposits comes from their primary transport process by bottom currents that are deflected by large landmasses and, thus, trend along continental slopes and shelves, where they are called boundary currents. More recently, contourites have been defined as 'sediment accumulations that have been emplaced or significantly affected by deep marine bottom currents' (Rebesco et al., 2014). 'Bottom currents' or, 'deep ocean currents' in turn, are described as currents that exist in 'deep waters', which is often considered to be below the thermocline (400–1000 m; Stow et al., 2018). As explained previously, most currents at these depths are thermohaline-driven geostrophic currents, but winds (e.g. internal waves and abyssal storms), and more importantly,

deep (internal) tides (Chelton & Schlax, 1996; Garrett & Munk, 1979; Thran et al., 2018) and other processes like gateway outflow water (e.g. Toucanne et al., 2007) are dominant in other places. The impact and relative importance of abyssal storms, internal waves and tides is poorly understood and may be negligible in many settings (Faugères & Mulder, 2011; Rebesco et al., 2008). In any case, thermohaline-driven geostrophic bottom currents are believed to be the dominant process at abyssal (>3000 m water) depths (Hernández-Molina et al., 2008; Shanmugam, 2017; Stow et al., 2018).

In addition to continuous processes, deep marine deposits are typically formed under the combined action of bottom currents and sediment/mixed-fluid gravity flows, which include turbidity currents and hyperpycnal flows (Figure 1; Mulder et al., 2003). The combination and interaction of these processes can generate a range of deposits like 'moat and drifts', which are bottom-current controlled systems that consist of depositional moat and erosional drift morphologies. (Rebesco & Stow, 2001). Other examples of bottom-current controlled deposits are 'plastered drifts' and 'sheeted drifts' (Faugères et al., 1999; Rebesco & Stow, 2001). All such bottom-current controlled systems are sometimes collectively referred to as 'bottom-current deposits' or 'contourites'.

2 | INTRODUCTION

Ocean bottom currents can erode, transport and redeposit sediments across the ocean floor. Whether deposition, erosion or neither occurs is believed to depend on local values for bottom current intensity and sediment availability (e.g. Faugères et al., 1993; Rebesco et al., 2014). For the development of contourites, bottom shear stresses can be too weak or too strong, respectively resulting in non-current driven deposition and bottom current erosion. Similarly, the amount of sediment supply in the deep ocean can be too limited (resulting in non-deposition). Lastly, areas with high values of sediment supply tend to be in close proximity to deep sea fans which are dominated by sediment gravity flows and turbidity currents (Rebesco et al., 2014) that often overprint the effects of weaker and more continuous bottom current deposits. Bottom currents are ubiquitous in our oceans so our ability to predict where and to what extent bottom currents affect ocean sediments is necessary for understanding deep ocean sedimentology and geomorphology. Predicting bottom current deposition and erosion also directly affects a range of practical topics like the construction and maintenance of ocean floor infrastructure (e.g. Stewart & Long, 2012), exploration of deep ocean resources like hydrocarbons (e.g. Zhang et al., 2019) and exploration for critical mineral resources

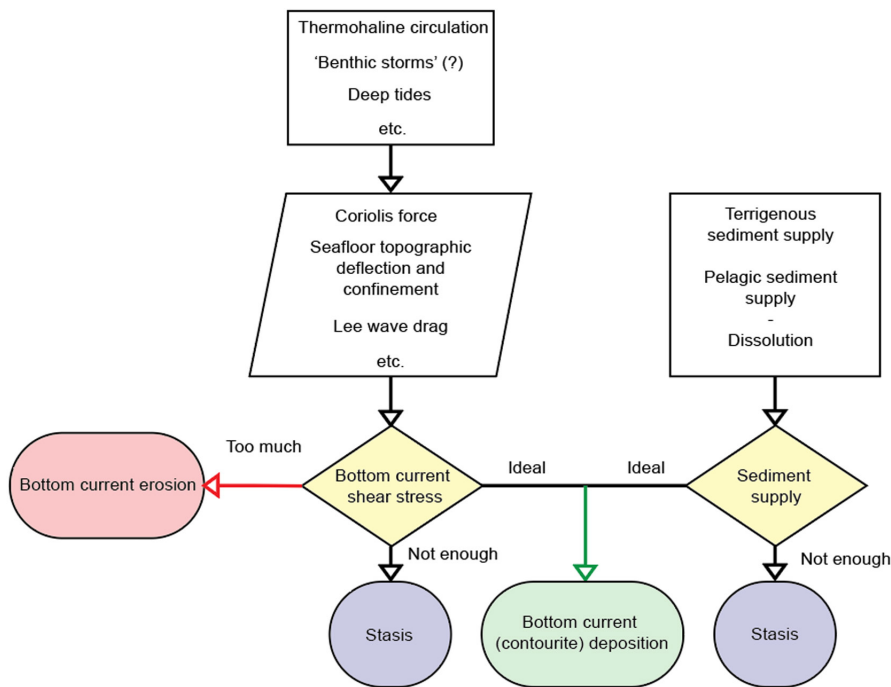


FIGURE 1 Schematic diagram showing the interactions of processes to form bottom current deposits. Thermohaline circulation and some other processes combine with Coriolis force to generate bottom shear stress. Sediment supply is mostly from terrigenous input transported into the ocean through gravitational processes. Bottom shear stress and sediment supply can combine locally to generate bottom current deposits. When bottom shear stress is too strong for deposition, erosion occurs. Adapted from Faugères et al. (1993). An illustration portraying a similar concept is in Rebesco et al. (2014).

(Peukert et al., 2018). Ocean floor mineral resources are also abundant, and a potential future target for economic extraction (Antrim, 2005). The spatial distribution of oceanic mineral resources can be linked to erosional ocean floor regions, which experience deflation of the sediments that surround much heavier ferromanganese and other metal-bearing nodules (Lonsdale & Malfait, 1974; Peukert et al., 2018). Ocean currents also play a role in the development of novel renewable and reliable energy resources like the recent pilot study that aims to power hydroelectric turbines by continuous geostrophic ocean currents (IHI Corporation, 2019). Deep ocean bottom current deposits also respond to environmental changes and are, thus, relevant to reconstructing conditions and events in (paleo) oceanography (Knutz, 2008; Rebesco et al., 2014). Sediments that have been effected by bottom currents are known to be some of the most important geological archives and have played a fundamental role in developing our understanding of global climatology and environmental change (e.g. Knutz, 2008). Being able to predict regions of deposition allows us to learn where such geological archives form and enables us to better evaluate their environmental history (Rebesco et al., 2014).

To better understand where and how bottom currents affect ocean floor sediments, researchers have used numerical modelling to link local (e.g. Bonaldo et al., 2016; Haupt et al., 1994) or global (Thran et al., 2018) bottom current intensities to the distribution of bottom current systems. This linkage is achieved by integrating observations of bottom current depositional features from sonar and seismic data (Claus et al., 2017), with insights from numerical ocean models (Thran et al., 2018). Existing

workflows have greatly benefitted our understanding regarding the effects of bottom currents on ocean deposits, but are limited because researchers often focus on bottom current intensities alone, without considering spatial variations in sediment supply. Sparse studies that have integrated oceanographic and sedimentological data, preceded the development of modern, more powerful numerical models, and had a regional focus (Haupt et al., 1994). In this study, we aim to improve on the state-of-the-art spatial predictions of bottom current deposition at a global scale. We aim to achieve this by integrating ocean floor geomorphology data with numerical bottom current intensity simulations and models of ocean floor sedimentation. Specifically, our aims are threefold: (1) quantify regimes of ocean bottom current deposition and erosion from various oceanographic and sedimentological data; (2) map the occurrence of bottom current deposition and erosion and compare this with existing information on bottom current depositional systems to evaluate the accuracy of our workflow (validation) and (3) formulate some generalized rules on where deposition and erosion tend to dominate across the oceans.

3 | METHODS

3.1 | Quantifying bottom shear stress

General circulation models can simulate deep ocean current intensities through computation of oceanic and atmospheric parameters, and thereby give information on bottom current velocities and shear stresses, even in

places where direct measurements are lacking. For example, the HYbrid Coordinate Ocean Model (HYCOM; Chassignet et al., 2009), is a complex numerical tool that computes the interaction between ocean overturning, surface ocean currents and deep ocean currents (Chassignet et al., 2009). The HYCOM model also incorporates Primitive Equations that simulate thermohaline conveyor current volumes and velocities, deep tidal activity, sea floor topography and rugosity and bottom current confinement and divergence due to coastline configurations (Chassignet et al., 2009). HYCOM integrates these aforementioned oceanographic principles with various geostrophic effects like Coriolis force and eddy circulation, to form a 'meso-scale eddy resolving' ocean model. Such a model can accurately quantify the impact of bottom currents on the ocean floor. As mentioned in the background section of this study, thermohaline bottom current conveyors are relatively deterministic, allowing accurate quantification of their intensities across the ocean using such complex ocean models like HYCOM. The HYCOM model is especially useful for our purposes since it is a hybrid model that incorporates both terrain following vertical levels in shallow ocean areas and isopycnal (having equal density) vertical levels in deep portions of the open ocean. Incorporating both of these two types of levels allows for a more accurate simulation of the interaction between stratified ocean currents and the ocean floor (Figure 2; Chassignet et al., 2009; Trossman et al., 2016). All model inputs are in the Supplementary Information 1.

To predict the dispersal of bottom current deposits, we use a single, realistic and representative model solution from the HYCOM model, which displays the amount of bed shear stress (often called bottom shear stress in the field of oceanography; see Trossman et al., 2016 for discussion) occurring on the seafloor in $1/12^\circ$ resolution (Trossman et al., 2016). Previous work has demonstrated that topography and ocean floor rugosity play important roles in controlling the amount of bottom current shear stress exerted, also an important variable for bottom

current deposition and erosion (Grant & Madsen, 1986). To accurately input bottom shear stresses, we use a HYCOM model run published in Trossman et al. (2016), which accounted for the effects of 'lee wave drag' from topographic blocking and ocean floor rugosity. The Trossman et al. (2016) HYCOM solution used in this study is a seasonally averaged model run, which reflects average yearly values of bottom current shear stress following a 13-year 'spin-up' or equilibration period. Real-world, measured, meteorological inputs from the U.S. National Oceanic and Atmospheric Administration (NOAA) have been applied across the model spin-up period. Further detail on the HYCOM model can be found in Chassignet et al. (2009) and more detail on the lee-wave incorporated run that is used in this study can be found in Trossman et al. (2013) and Trossman et al. (2016).

All datasets are global coverage and are converted to a numerical matrix with equal dimensions and map projection (equiarectangular).

3.2 | Quantifying sediment availability

Although sediment is deposited across the entire ocean floor, many places, such as near mid-ocean ridges have very little sediment accumulation (Stow et al., 2008; Straume et al., 2019). In the case of mid-ocean ridges, this low sediment supply is because of their location far from terrestrial and shallow marine sediment sources combined with limited input from sediment production in the water column (Stow et al., 2008). Because of these factors, the majority of mid-ocean ridges are devoid of contourites and bottom current deposits (Claus et al., 2017), even in areas where bottom shear stress is significant. To account for variable sedimentation rates across the ocean floor we collect global information on the sedimentation rates across the abyssal plain. Values of oceanic sediment thickness have been accurately determined for the entire ocean floor in a detailed sediment thickness map called GlobSed

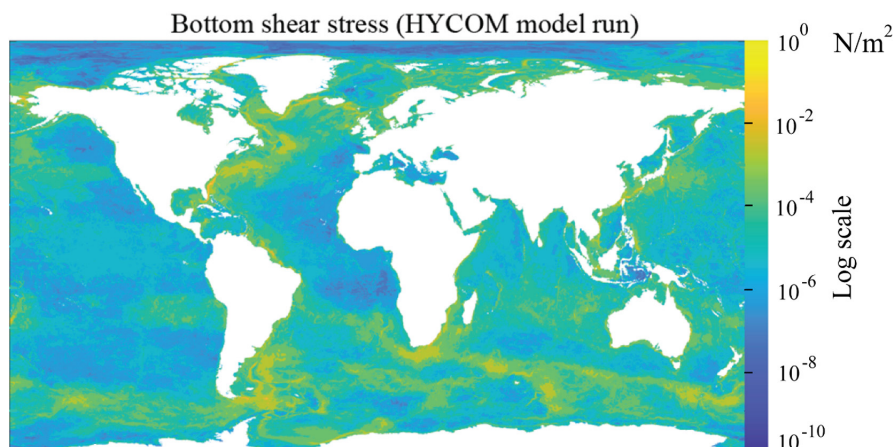


FIGURE 2 Map displaying the bottom shear stress input used in this study. Bottom shear stress is modelled using the HYCOM model (Chassignet et al., 2009) and incorporated topographic lee-wave drag (Trossman et al., 2016). Log scale, along the right margin of the diagram, refers to the logarithmic scale for the values portrayed in the Y-axis.

(v3) (Straume et al., 2019), is constructed from interpolating sediment column thicknesses obtained from seismic data and ocean drilling (Straume et al., 2019). However, sediment thickness is to a large extent, controlled by the depth to the base of the oceanic lithosphere, since older portions of the seafloor have simply had more time to collect sediment. To achieve an accurate estimate of oceanic sedimentation rates, we integrate the ocean sediment thickness models with a lithospheric age model. Local ages for the oceanic lithosphere are mapped from spreading rates and distances from the nearest spreading ridge (Müller et al., 2008). By dividing local values for sediment thickness (m) with local values for lithosphere age (kyr), the sedimentation rate across the ocean is calculated (m/kyr; Figures 3 and 4).

3.3 | Training datasets and the contourite atlas

Creation of a globally predictive model of conditions conducive to contourites deposition requires that we train the model using information from known and well-documented areas of contourite deposition. The location and extent of bottom current deposits have been compiled and published in a 'contourite atlas' (Claus et al., 2017). The atlas shows a series of polygons that delineate the location and extent of mapped contourites across the world's oceans (Figure 5). These data have been collected from countless deep sea exploration surveys across several decades of ocean exploration. Since this study is focused on predicting bottom currents specifically, various polygons that we interpret from the literature as not being bottom current deposits are removed from the contourite atlas compilation. For example, the 'Dongsha sediment wave fields' (Gong et al., 2015) have many geometric characteristics that we interpret as being associated with 'cyclic steps', which are not thermohaline bottom current deposits, but rather supercritical flow structures formed by gravitational currents (Gong et al., 2015; Slooman & Cartigny, 2020). The criteria that we use to separate thermohaline features from cyclic steps are listed in Beelen et al. (2021). The data we used to investigate the authenticity of features mapped in the contourite atlas are publicly available sonar data compiled in the GEBCO data accumulation project (Kapoor, 1981). A list of our adjustments to the contourite atlas with non-bottom current controlled polygons removed is in the supplementary Information 2.

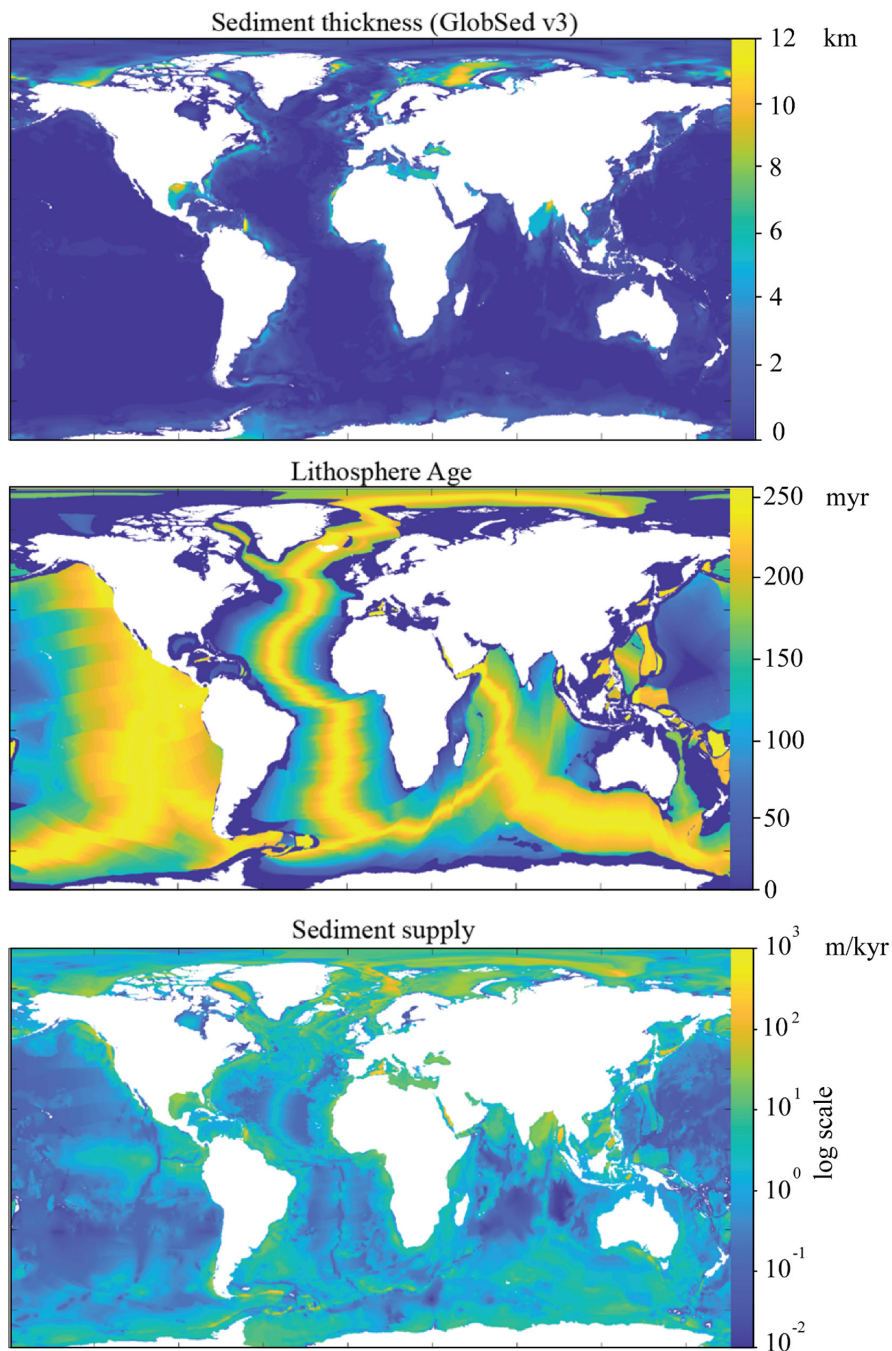
To achieve a globally representative prediction, we chose several geographic subsets of bottom current occurrences documented in the contourite atlas map and well supported in other literature and used these subsets as 'training data', to show us under which regime bottom

currents tend to form. Three training data subsets have been defined termed T1, T2 and T3. T1 is the smallest subset, which is a single contourite depositional and erosional system east of Greenland called the Eirik Drift. This system is relatively diverse, having both erosional and depositional components (Hunter et al., 2007). The Eirik Drift has been mapped across many sonar and drill core studies (Hunter et al., 2007) so the geographic extent of this contourite has been accurately constrained with limited uncertainty. The second subset used as training data; T2, is by far the spatially largest (Figure 6) as it covers most of the western side of the Atlantic Ocean. A large number of sediment drifts are present here, many of which are mapped in detail (e.g. Hollister & Heezen, 1972). The final subset; T3 is a region with abundant sediment drifts in the northern Atlantic Ocean, which has been investigated in the context of bottom current depositional features across many studies that have taken place over the course of several decades (e.g. Hollister & Heezen, 1972). Several well-studied thermohaline bottom current depositional features occur within this subset, such as the Feni, Gardar and Hatton Drifts (Table 1) (Hollister & Heezen, 1972). All training data inputs are in the Supplementary Information 3.

3.4 | Defining cutoff values for bottom current deposition and erosion

The likely regime for contourite deposition is delineated by defining four 'cutoff values' termed A, B, C and D. Here, A is defined as the minimum sedimentation rate for contourite deposition, B is the maximum sedimentation rate for contourite deposition, C refers to the minimum shear stress for contourite deposition and D is the maximum shear stress for contourite deposition. The values for A, B, C and D are determined by computing a wide range of input values and then defining the optimum. The range of input values is the total range of sedimentation rates and shear stresses that occurs within the contourite atlas polygons of the training data subset. This total input value range is divided into 100 increments to give an array of 100 possible values for A, B, C and D. Division into 100 increments is chosen as to achieve a high-enough resolution but allow for limitations of the computing speed (see: Discussion, sensitivity analysis). To define the correct values for minimum and maximum sedimentation rate, all possible combinations of the A and B arrays are merged into a matrix whereby $A < B$, resulting in a 2×4950 ($4900 = 100^2/2 - 100$) matrix that contains all combinations of A and B and, thus, all numerical ranges that are considered. A score is calculated for each numerical range by calculating the percentage of correctly predicted $1/12^\circ$ grid cells for a given numerical range and then subtracting

FIGURE 3 All data inputs used for the sediment supply inputs for the prediction. Top: Ocean Sediment thickness map from the GlobSed v3 model (Straume et al., 2019). Middle: Lithosphere Age map from Müller et al., 2008. Bottom: Sediment supply map constructed by dividing values of sediment supply with corresponding values of lithosphere age. Log scale refers to Logarithmic scale for the values portrayed in the Y-axis.



it by the percentage of incorrectly predicted grid cells for a given numerical range. Here a correctly predicted grid cell is defined as ‘a grid cell with values between A and B that spatially corresponds to a grid cell that sits inside a contourite atlas polygon’ (Figure 7). Wrongly predicted grid cells are defined as: ‘grid cells with values inside the numerical range between A and B that sit outside of a contourite atlas polygon’. This method maximizes the number of depositional grid cells that correspond to depositional regions in the contourite atlas while accounting for overprediction by subtracting the percentage of depositional grid cells that do not correspond to depositional regions in the contourite atlas. Values for A and B that

define the numerical range with the highest score are then determined to be the optimal values. This workflow is applied to find the optimal range for sediment supply (values A and B) and then in the same way to find the optimal numerical range for shear stresses (values C and D; Table 2). The code used for training the model and rendering the prediction are in the Supplementary Information 4.

3.5 | Sensitivity analyses

To determine the accuracy of the methodology, two sensitivity analyses are performed: First, values that are adjacent

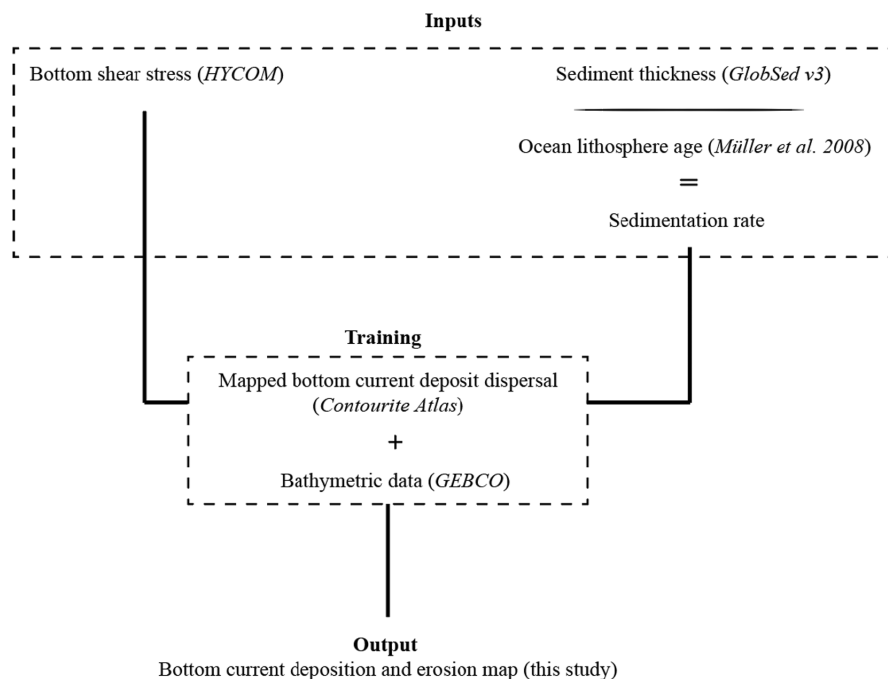


FIGURE 4 Schematic diagram displaying the various inputs and training dataset used to generate the prediction.

to the highest score for A and B differ by only one numerical increment. These slightly different values are plotted in addition to the highest score to quantify the difference across a single numerical increment. Results from this analysis show that a single numerical increment (1/100 of the total range considered) results in a < 1% different prediction and is, therefore, not significant. Choosing a different increment value (e.g. 1/1000 or 1/200) would come at a cost of requiring exponentially more computing resources but would not result in a significantly different prediction.

The second sensitivity analysis revolves around the training data. Three training subsets that differ in size and location are outlined (T1, T2 and T3; Figure 6). By examining the resulting differences, the model's sensitivity to the chosen training data inputs can be estimated. This analysis shows that a pick of training data has a significant effect on the model output. In choosing the training data input for the final prediction, a balance is struck between choosing large, well-mapped swatches of the ocean floor while keeping large surfaces outside of the training input to allow for model validation. Based on this logic, we pick a large region of the Western Atlantic Ocean as the training for our best prediction (T2, Figure 6).

4 | RESULTS

4.1 | Predicting bottom current deposition and erosion

Frequency histograms of bottom shear stress and sediment supply indicate that these parameters are lognormally

distributed across the ocean floor (Figures 5 and 8). Bottom shear stress conditions within the thermohaline contourite atlas polygons are compared with bottom shear stress conditions outside of the mapped extent of contourites and bottom current deposits. As expected, bottom shear stresses within polygons (signifying conditions of bottom current deposition) are significantly higher, on average 568% higher than outside of polygons. A similar result is obtained when considering sediment supply, which is on average 240% higher inside the contourite atlas polygons than outside of the polygons. These values show that bottom current deposits tend to form in areas with above-average values of bottom shear stress and sediment supply, thereby supporting notions from Faugères et al. (1993); Rebesco et al. (2014) and a key assumption in this study (Figures 1 and 4).

Regions within the cutoff values for sediment supply and bottom shear stress (see Methods section) are predicted to have bottom current deposition and are coloured in the map prediction as swaths of green, (Figure 9; Supplementary Information 5). Within our map prediction, further information on bottom current deposition is provided by displaying the product of shear stress and sediment supply (Figure 9). Bottom shear stress multiplied by sediment supply ($\text{N/m}^2 * \text{m/s}$) has unit N/ms or alternatively kg/s^3 . Such a parameter is a measure of 'energy flux density', which is not directly intuitive or useful but since higher values of sediment supply and shear stress have been shown to correlate with mapped contourites, we use this concept to add further detail to regions that are predicted to have bottom current deposition (Figure 9).

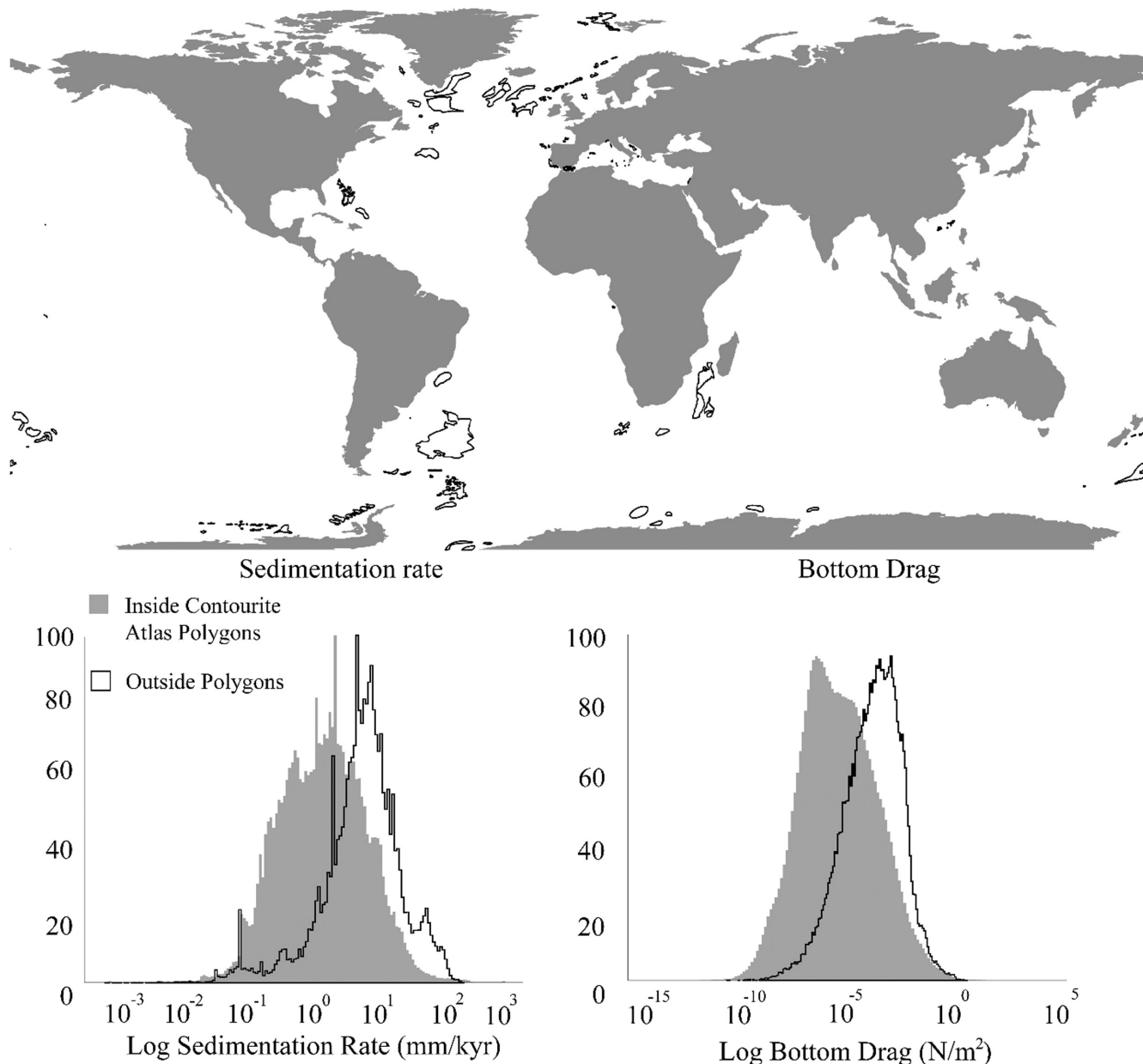


FIGURE 5 Top: World map showing polygons from the contourite atlas (Claus et al., 2017). Frequency histograms showing values for sedimentation rate (bottom left) and values of bottom shear stress (bottom right) across the world's oceans. Data represented in the filled grey histograms represent the entire ocean. Data represented by the transparent histograms represent values inside the contourite atlas polygons and, thus, represent sediment supply and shear stresses across mapped contourites. Although there is a lot of overlap in the data, contourites prolific regions of the ocean tend to have significantly higher amounts of sediment supply and bottom shear stress than regions of the oceans where no contourites have been detected. Logarithmic scale for the values portrayed in the X-axis is shown on the left side of the graphs.

Portions of the ocean that have values for bottom shear stress that exceed the maximum cutoff (cutoff D) are coloured in red (Figures 8 and 9). Cutoff D refers to the maximum bottom shear stress associated with deposition and separates the regime of deposition from a regime of erosion. Bottom current erosion is predicted to occur regardless of the amount of sediment supply. Bottom current erosion is graphically displayed on the map prediction as various shades of red which

correspond to the local intensity of bottom shear stress (Figure 9).

Portions of the ocean that are below the minimum amount of sediment supply (cutoff A) or the minimum amount of bottom shear stress (cutoff C) are predicted to have stasis and are coloured in blue (stasis; Figure 9). Values that exceed the maximum cutoff value for sediment supply are predicted to be dominated by non-bottom current-related processes and are also predicted to have

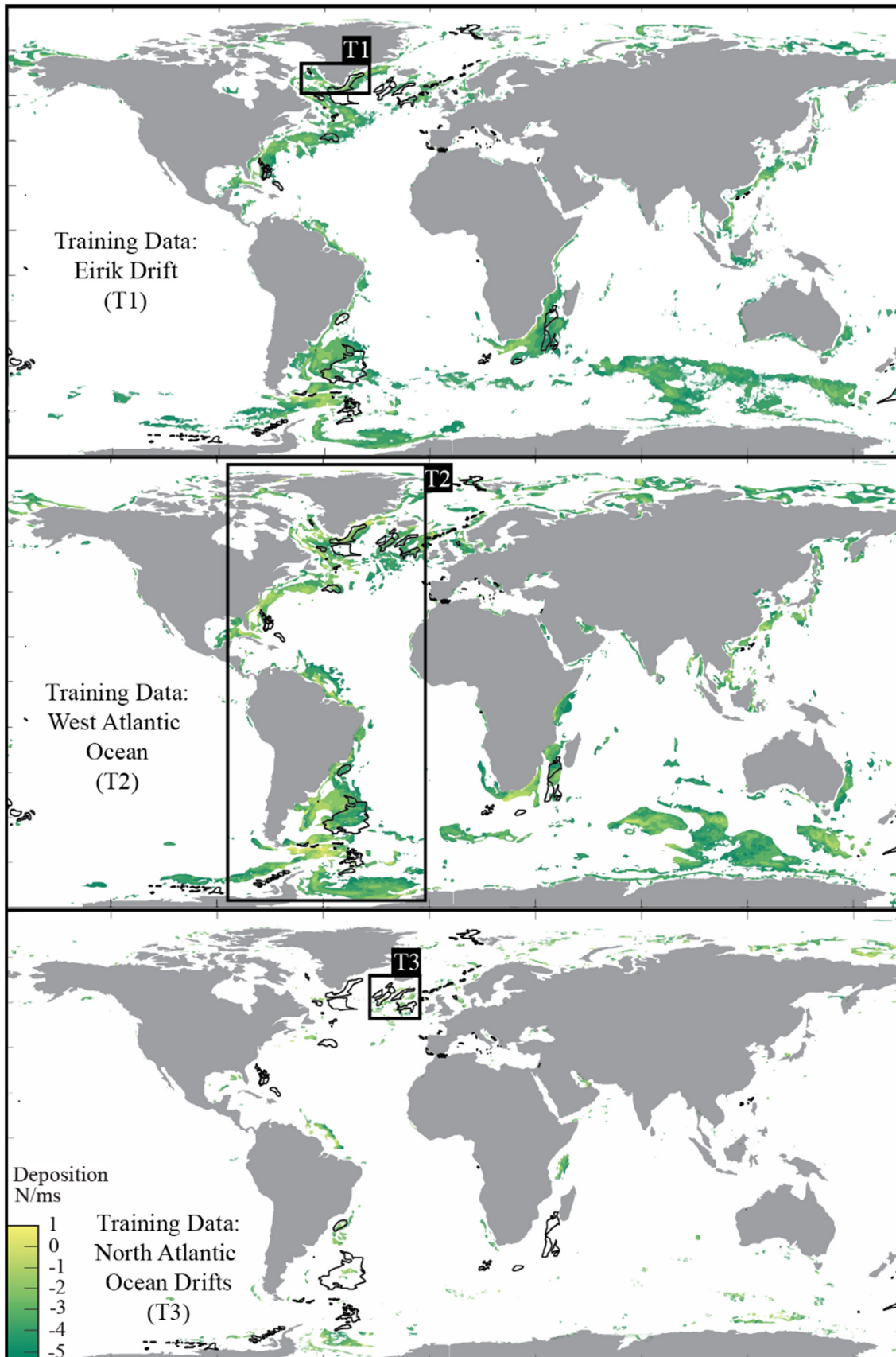


FIGURE 6 Contourite atlas published in Claus et al. (2017). Locations of contourites and bottom current deposits in this dataset are determined from direct observations using sonar and drill core data. Black polygons represent the mapped extents of contourites and abyssal dunefield. Black boxes titled T1, T2 and T3 show the outlines of the various Training datasets.

TABLE 1 Dataset used as inputs for the prediction presented here.

Dataset type	Dataset	Source
Bottom shear stress	HYCOM: HYbrid Coordinate Ocean Model model run	Chassignet et al. (2009) Trossman et al. (2016)
Sediment thickness	GlobSed v3	Straume et al. (2019)
Ocean lithosphere age		Müller et al. (2008)
Bottom current deposit dispersal	Contourite atlas	Claus et al. (2017)
Bathymetry	GEBCO: General Bathymetric Chart of the Oceans	Kapoor (1981)

bottom current stasis (Figure 8). According to our map prediction, around 12% of the ocean surface is predicted to have deposition by bottom currents, and 1% of ocean surface is experiencing erosion by bottom currents. The remaining ocean floor (87%) is predicted to have bottom current stasis.

4.2 | Model validation

The accuracy of the prediction can be judged in two ways. First, we list the percentages of correctly predicted grid cells per training input (Table 3).

Second, the accuracy of our map prediction can be judged by comparing predicted plan-form geometries of contourites to mapped plan-form geometries. Two regions of the ocean floor are considered here which are the Gulf of Cadiz and the Alboran Sea. Both of these areas lie outside of the training data extent (T2) and are especially well mapped across many sonar and drill core studies.

4.2.1 | Gulf of Cadiz

The Gulf of Cadiz contourite system is driven by Mediterranean Outflow Water (Baringer & Price, 1999). It exhibits erosional channels that were formed by strong bottom currents and channel-adjacent contourite depositional systems (Figure 10; Hernández-Molina et al., 2016). Although this is a relatively small system on an oceanic scale, it has received a lot of research attention and is well mapped using the abundant collection of sonar and sediment core data (Gonthier et al., 1984; Llave et al., 2007; Sánchez-García et al., 2009). Comparison between our map prediction and the known contourites in the Gulf of Cadiz indicate that our model has correctly predicted the erosional moat near the strait of the Gibraltar Strait and the adjacent drift to the north of this feature. The model has also correctly predicted a field of stasis toward the south and southwest of the Gulf of Cadiz (Figure 10).

4.2.2 | Alboran Sea

Another test case for model accuracy is the Alboran Sea (Ercilla et al., 2016). Like the Gulf of Cadiz, this area lies outside of the training data extent (T2) and is, thus, suitable for model validation. Comparison between our map prediction and the known distribution of contourites the Alboran Sea shows that the location and extent of various mapped sheeted drifts have been predicted accurately. Some examples include the Motril Basin drifts in the north of this system as well as the Cueta and Al Hoceima systems which are located on the southern edge of the Alboran Sea. Elongated and separated drifts on the Alboran and Djibouti ridges are oriented diagonally across the Alboran Sea and are also predicted accurately in terms of their planform geometry (Figure 10).

5 | INTERPRETATIONS

5.1 | Depositional zones

Some zones with prominent bottom current deposition identified in the model are in the northern Atlantic Ocean (e.g. Gloria, Eirik, Björnsson, Gardar and Feni drifts, McCave & Tucholke, 1986; Flood et al., 1979), the Argentine Basin (Zapiola Drift), the Mozambique Channel and the Agulhas current systems (e.g. Breitzke et al., 2017), the Australian and Indonesian continental shelves, the Bering Sea and areas of the Southern Ocean (e.g. Cosmonaut Drift and Larsen Sea Drift, Rebesco et al., 2014; Figure 9). In general, areas of bottom current deposition tend to occur on continental slopes, where relatively abundant sediment is derived from the land, and significant topography is present to amplify shear stresses exerted by bottom currents. Examples of these areas are the Antarctic circumpolar currents, the North Atlantic boundary current and the Mozambique undercurrent. Another type of area with abundant bottom current deposition are abyssal regions with significant intermediate-to-bottom water downwelling. These

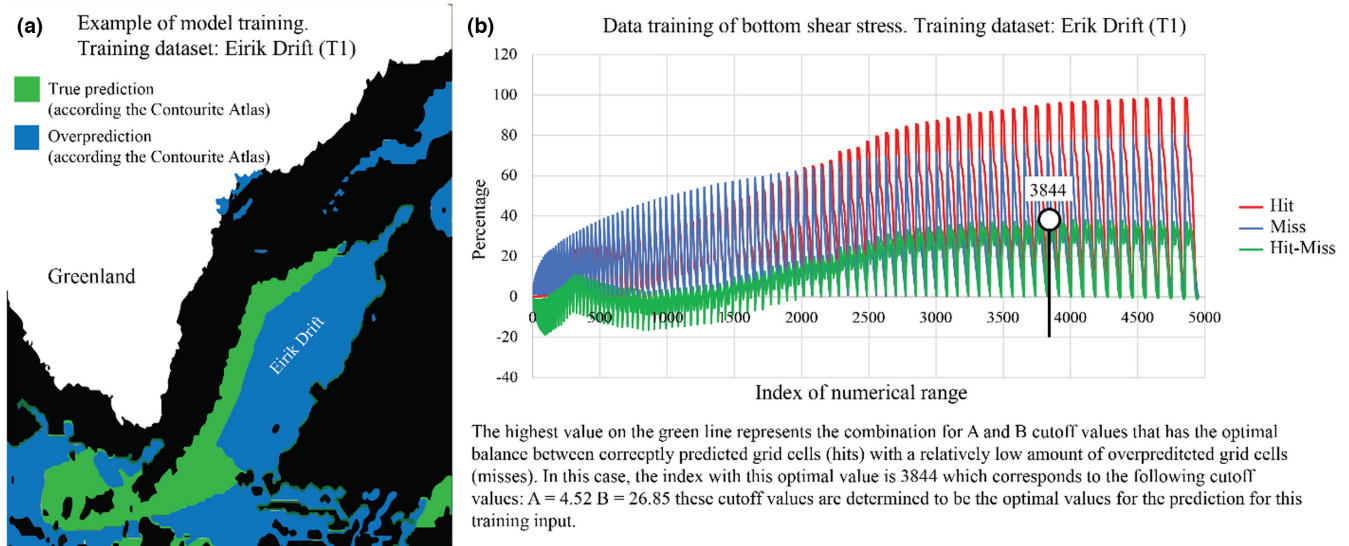


FIGURE 7 (a) Schematic figure demonstrating the workflow used to define the ideal shear stress cutoff values for bottom current deposition. For any numerical increment, predicted grid cells that correspond to mapped contourite deposits in the contourite atlas (Claus et al., 2017; light green) are counted. Overpredicted grid cells (dark blue, which do not correspond to mapped contourite deposits in the contourite atlas) are also counted. The set of inputs that has the highest proportion of ‘correctly’ predicted grid cells while having the least ‘overpredicted’ grid cells within the training data subset is determined to be the best set of inputs for the prediction. (b) Graph showing the percentage of correctly predicted grid cells (X-axis, blue) as a function of each numerical increment (X-axis). Percentage of incorrectly predicted grid cells as a function of numerical increment is shown in red. Training dataset used here is T1, Eirik Drift. The green line shows the blue line minus the red line and represents the most accurate prediction with the least overprediction. The highest values on the green line (in this case, value 3844 corresponds to the numerical increment with best estimate values for minimum shear stress for bottom current deposition and maximum shear stress for bottom current deposition. These values are combined with sedimentation rate values calculated in the same way. Based on the resulting cutoff values, the map prediction is constructed.

Cutoff value	Meaning	Numerical value (based on West Atlantic training data subset)	Unit
A	Minimum sediment supply for bottom current deposition	8.14	mm/kyr
B	Maximum sediment supply for bottom current deposition	27.15	mm/kyr
C	Minimum bottom shear stress for bottom current deposition	0.00066	N/m ²
D	Maximum bottom shear stress for bottom current deposition	0.27	N/m ²

TABLE 2 Prediction cutoff values following model training on the West Atlantic training data subset (T2).

Note: Values in the legend are in logarithmic scale.

areas of downwelling, which are commonly driven by barotropic vortices, occur irrespective of ocean pressure and temperature gradients. In these regions, sediment is confined, and vigorous bottom currents can rework

this sediment into extensive wavefields like the Zapiola Drift Abyssal Wavefield. The Zapiola system is driven by barotropic vortex currents, which generate a vast wavefield containing some bedforms up to 125 m high.

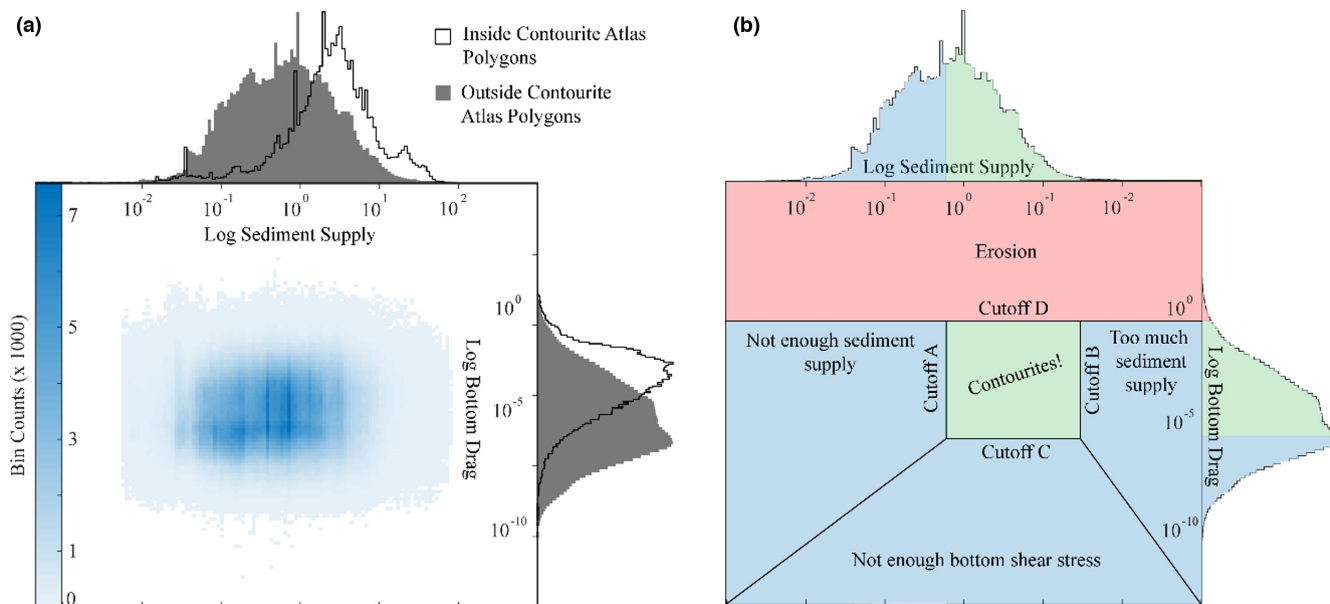


FIGURE 8 (a) Density scatter plot with Sediment supply on the X-axis and bottom shear stress on the Y-axis (both are log axes). Both parameters are lognormally distributed across the ocean. Density scatter shows the frequency of data points with a certain value. Histograms show the same data. Black polygon shown sediment supply and bottom shear stresses inside the mapped polygons of the contourite atlas, showing contourites form in areas with relatively high sediment supply and bottom shear stress. (b) Same as in A but with the various regimes that indicate bottom current deposition, erosion and stasis visualized. Log scale refers to Logarithmic scale for the values portrayed in the relevant axis.

These moving abyssal bedforms are some of the largest bedforms on Earth (Volkov & Fu, 2008). In addition to abyssal wavefields, bottom current deposition can also occur in abyssal regions with significant topography like the Kerguelen Plateau and the Zealandia submarine continent (Figure 9). In these areas, topographic obstacles like seamounts locally amplify bottom shear stresses, causing bottom current deposits to form onto or adjacent to these features.

5.2 | Erosional zones

Major zones of bottom current erosion are shown by the model to occur off the east coast of the United States, such as the area around the Blake Plateau, located offshore east of Florida (Figure 11). This area experiences very powerful bottom currents: the Florida Current or Southern Gulf Stream Boundary Current (Spall, 1996), which in some places exert 20 N/m^2 (compared with the ocean floor average of 0.00378 N/m^2), of bottom shear stress onto the seafloor (Trossman et al., 2016). The bottom current system in this area continuously removes and redistributes sediment, developing an enormous depositional system called the Blake Ridge, which occurs in association with a large erosional zone (Figures 12 and 13). Other major erosional areas are found west of the Zapiola Drift that trend along the Argentinian Continental Shelf, areas

around the Agulhas Boundary current, the Kerguelen Plateau, the Bering Straits and areas south of the New Zealand Plateau. The presence of powerful continuous geostrophic boundary currents along the ocean's margins is revealed in the topographic character of the margin. The seafloor topography made rugose by frequent gravity failures running upslope to downslope, perpendicular to the margin will be smoothed by the presence of powerful along-margin currents. In contrast, margins lacking such seafloor 'smoothing' by boundary currents will retain their seafloor rugosity, scarred by numerous gravity flows (Figure 11).

Zones of deep water erosion are also common in sea straits, where geostrophic or non-geostrophic but equally persistent deep, tidal currents are confined and amplified. Some examples are the Mozambique Strait, Bering Strait and the Gulf of Cadiz (Figures 9 and 13). Modelling in this study suggests that the English Channel has both areas of deposition and erosion, but appears to be dominantly erosional in its central, narrowest region where amplified ideas are known to develop furrows (Flood, 1981; Figure 14).

5.3 | Zones of bottom current stasis

According to our map prediction, 87% of the ocean floor is predicted to have bottom current stasis, which is a state of neither deposition nor erosion by bottom

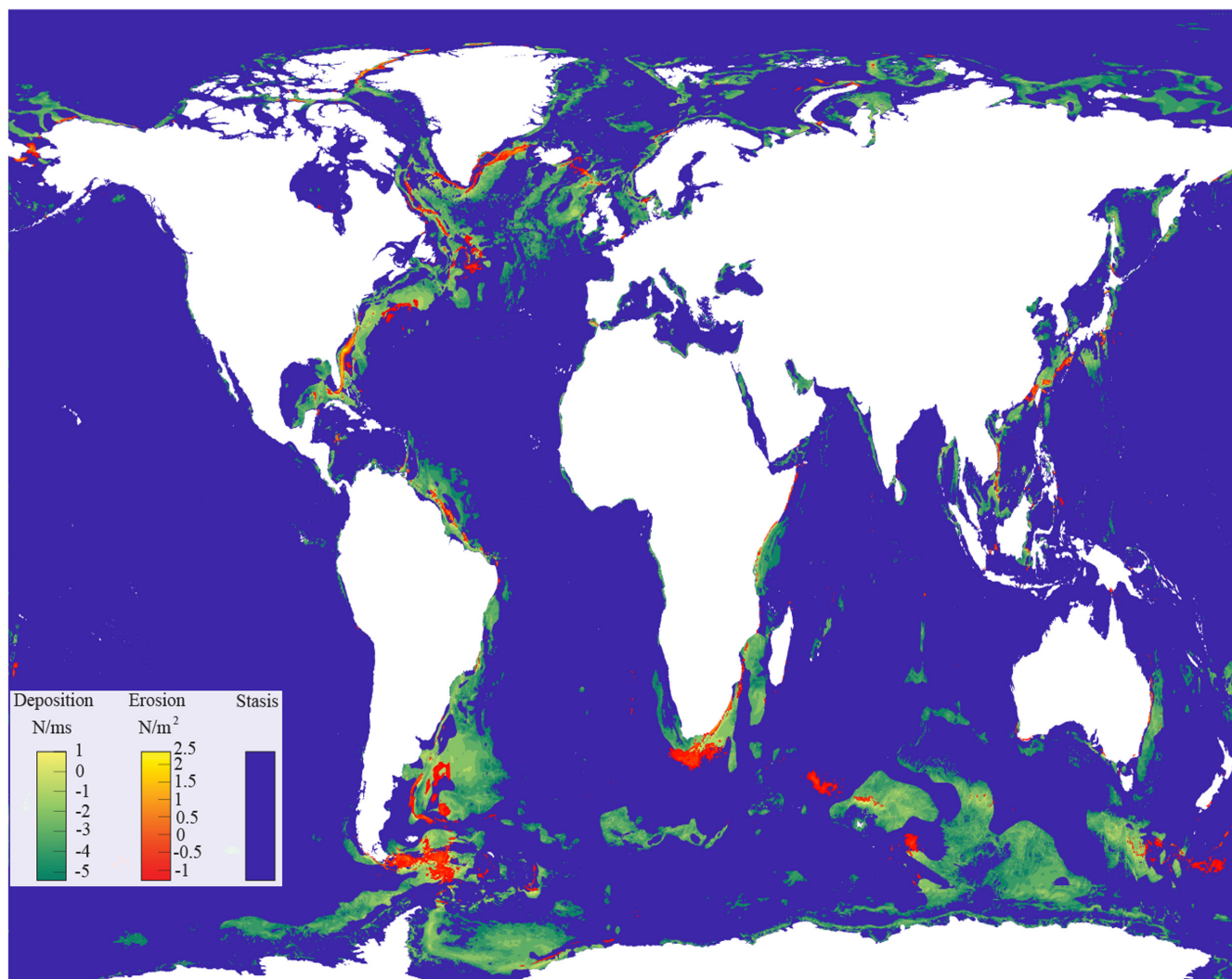


FIGURE 9 Map prediction showing bottom current deposition (green) and erosion (red) and stasis, neither deposition nor erosion by bottom currents (blue). Input for this prediction is training dataset T2, which covers most of the Western side of the Atlantic Ocean. Various shades of green represent differences in the multiplicative of sediment supply and shear stress (energy flux density). Shades of red represent the amount of bottom shear stress. Note that deposition and erosion are in a different unit. All values in the legend are in logarithmic scale.

TABLE 3 Simple validation showing percentages of correctly predicted bottom current deposits (according to mapped contourites from the Claus et al., 2014 'contourite atlas').

Training data	Percentage of correctly predicted grid cells
T1, Eirik Drift	67
T2, Western Atlantic	86
T3, North Atlantic	43

Note: See Figure 9 for extents of training data inputs.

currents and can be separated into three separate types (Figure 8). Firstly, there are zones of too much sediment supply which account for about 4% of the ocean surface

area (Brown, Figure 15), these zones represent regions that are dominated by gravitational processes like turbidity currents (Figure 1; Faugères et al., 1993; Rebesco et al., 2014). Regions such as this are nearby the mouths of large rivers where they form roughly lobe-shaped regions of very high sediment supply that probably represent the offshore portions of large deltas. Other regions that have very high sediment supply are some continental shelves and slopes and basins that are surrounded by land masses like the Mediterranean Sea and the Arctic Ocean (Table 4; Figure 9). A second type of environment characterized by bottom current stasis are areas that lack the sediment supply to form contourites and abyssal wavefields (light grey, Figure 15; Faugères et al., 1993; Rebesco et al., 2014). Such areas are common on the abyssal plain where there is limited sediment input from land-derived sources. Sedimentologically, these regions do collect some

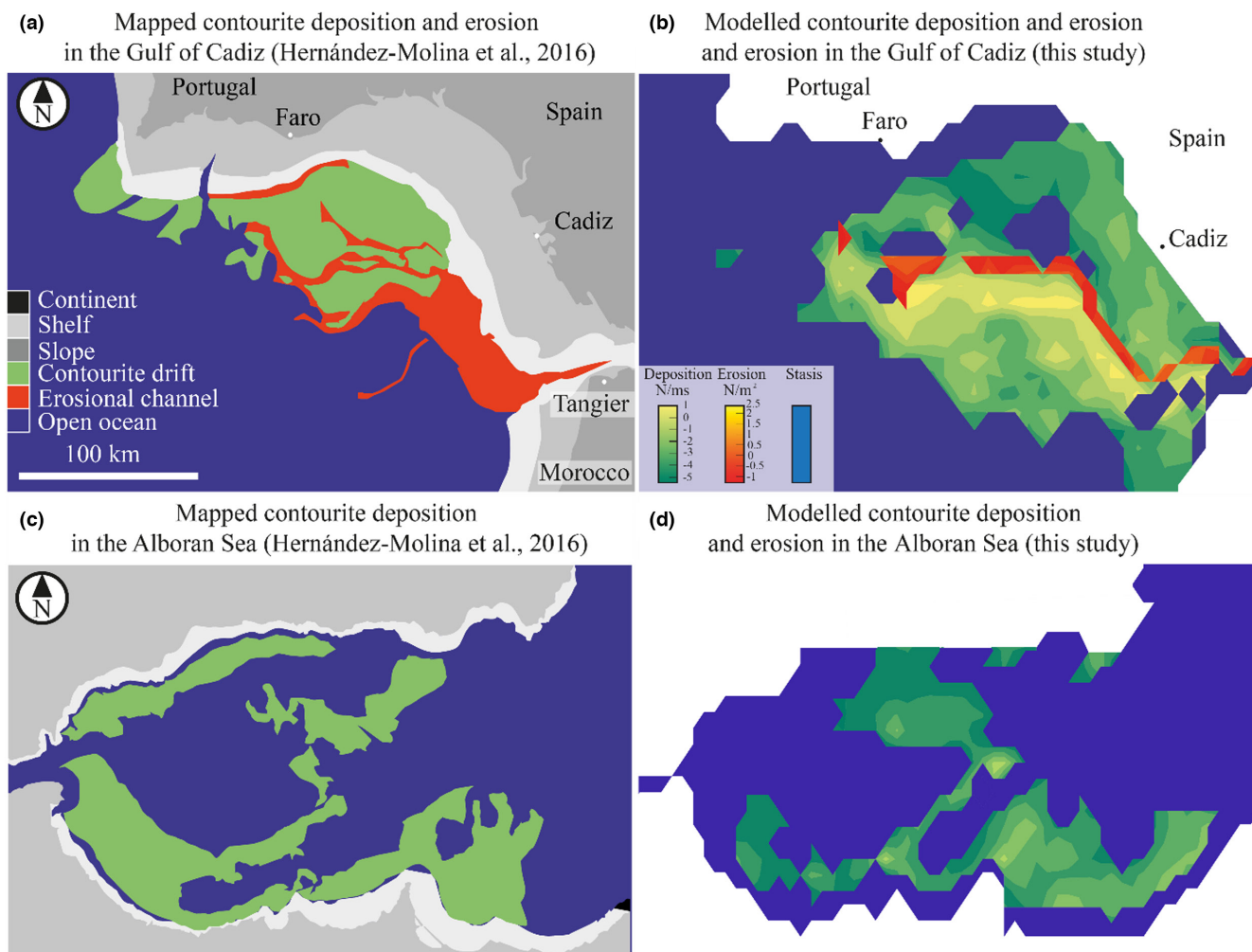


FIGURE 10 Validation of the map prediction through comparison of plan-form extents and geometries of contourites that are outside of the input training data. (a) map prediction of the Gulf of Cadiz shows an erosional moat surrounded by contourite depositional systems flanking the moat. (b) Mapped contourite depositional system also in the Gulf of Cadiz, adapted from Hernández-Molina et al. (2016) shows a similar erosional moat but with mostly deposition on the northern flank of the moat. (c) map prediction of the Alboran Sea contourites shows a distribution of contourites that is similar to the mapped extents of plastered and elongated drifts according to Ercilla et al. (2016). Values in the legend are in logarithmic scale.

material from the water column and are interpreted to result in the formation of ‘condensed pelagites’ (light grey Figure 15; Fabbi et al., 2016; Hüneke et al., 2021). Third, there are areas that collect enough sediment for contourite deposition but lack the bottom shear stress to form deposits. Such areas, which are common on the abyssal plain and near mid-oceanic ridges are interpreted to have dominantly pelagic deposition through the quite settling of sediment whereby no continuous or intermittent current process has any significant effect. Overall, stasis of bottom current processes is common in regions that are very far from continents, where no terrestrially derived or reworked sediments are available, such as over mid-ocean ridges (Figure 15). Areas of significant deepwater formation, such as north of Iceland (Figure 9) or the Weddell Sea near Antarctica (Figure 9) also have marked zones of

stasis, due to a lack of bottom currents passing across the ocean floor in these regions. Instead, water masses move vertically downward in these areas, and the HYCOM model run used here, suggests that such vertical movement of water masses coincides with a limited amount of bottom shear stress on the ocean floor (Chassignet et al., 2009; Trossman et al., 2016). Another common area of stasis due to a lack of bottom shear stress, are the ocean’s continental shelves, for example, off the east coast of the United States (Figure 12). A lack of bottom current activity on continental may occur because deeper thermohaline bottom currents remain on the abyssal plain, below or on the toe of the continental slope, and tend to take the path of least resistance and, thus, avoid getting forced up to shallower continental shelves (Rebesco et al., 2014). Exceptions to the limited deposition of bottom currents

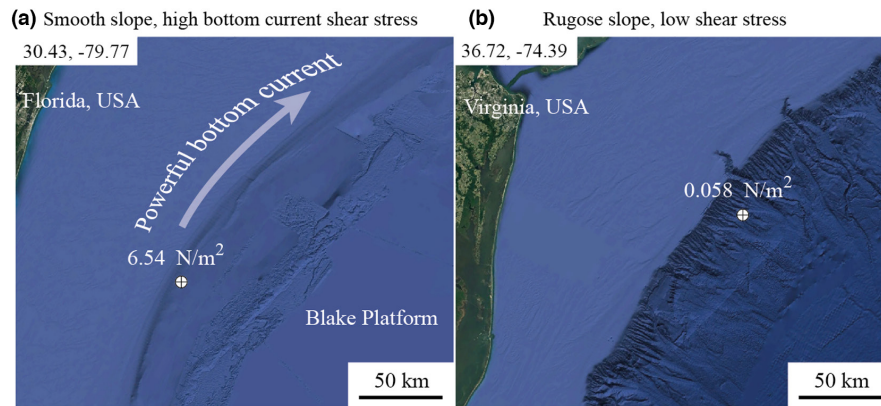


FIGURE 11 Bathymetry data of two near-adjacent continental shelf and slope systems off the East Coast of the United States. (a) The continental slope adjacent to the Blake Plateau shows a smooth texture. The seafloor topography of this region is smoothed out by erosion due to high shear stress bottom currents (6.54 N/m^2). (b) Continental slope ~ 1000 km north of the Blake Ridge along the same margin showing an abundance of slope incisions. This region lacks erosional bottom currents and, therefore, has low bottom shear stress. This preserves the seafloor rugosity in this area that is caused by downslope turbidity current erosion.

exist where continental shelves have high-enough shear stress conditions to develop deposits. Such continental shelf bottom shear stress can be caused by deep tides that are sometimes amplified near the coast or on the shelf (Davis & Dalrymple, 2011; Rebesco et al., 2014). The amount of tidal shear stress on continental shelves is contingent on the depth of the shelf and the amount of tidal energy in the area. The amount of tidal energy, in turn, is mostly controlled by the shelf's relative position to the nearest amphidromic point and the local coastline shape and orientation (Davis & Dalrymple, 2011). An example of a continental shelf that is experiencing bottom current deposition and erosion is offshore Florida (Figure 12). A fourth type of deep water region that commonly experiences stasis are deep, partially, or completely enclosed basins like bays or seas, such as the Black Sea (Figure 9), the Bay of Bengal (Figure 9). These areas are generally bypassed by global thermohaline bottom current conveyors. Other enclosed seas that have bottom current deposition and erosion are the Adriatic Sea (Figure 9; Pellegrini et al., 2016) and the Northern portion of the South China Sea (Figure 9; Chen et al., 2019).

6 | DISCUSSION

6.1 | Mixed systems

Terrigenous sediment supply in deep ocean systems is dominantly provided through gravitationally driven processes like turbidity currents (e.g. Faugères et al., 1993, see background section). Bottom currents can deflect these sediments on their way to the ocean floor and also winnow and displace the sediments after they have settled (Rebesco et al., 2014). In all cases, it is the synergistic action of

gravitational processes and bottom current processes that combine to develop most types of bottom current deposits. Each deep ocean deposit, therefore, develops under a unique balance of gravitational versus bottom current processes. For example, turbidite channel lobe systems (e.g. Savoye et al., 2009) are formed almost exclusively under the action of gravitational processes, while abyssal wavefields form almost entirely under the action of continuous bottom currents (e.g. Lonsdale & Spiess, 1977). In most cases, however, deep ocean deposits form in an environment that lies somewhere within a continuum between gravitational and continuous bottom current processes. These systems that form under the influence of both types of process can qualify as so-called 'mixed systems' (Fonnesu et al., 2020). Studies on mixed systems (e.g. Mulder et al., 2008) have variously found that the dominant process regime plays a key role in defining the overall geometry of the contourite deposit, both in terms of its 3D architecture as well as its planform geometry (Figure 16). Planform geometry is, therefore, one of the criteria that can be used to classify different types of continuous current deposits and the planform predictions of bottom current depositional and erosion can be used to examine various types of contourite systems (Figure 16). For example, moat and drift contourite systems are fed with sediment sourced from continental shelves, whereby the coarse-grained component is deposited in a moat occurring proximal to and running parallel to the toe of the continental slope (Faugères et al., 1999). In these moats, fine material is winnowed, and can, thus, be classified as an erosional zone (Figure 16). Moat and drift mixed systems also have a 'drift' component, which is generally comprised of finer-grained material that is carried further basinward by continuous geostrophic currents (Miramontes et al., 2020). Planform geometries of moat and drift systems are visible on our map prediction

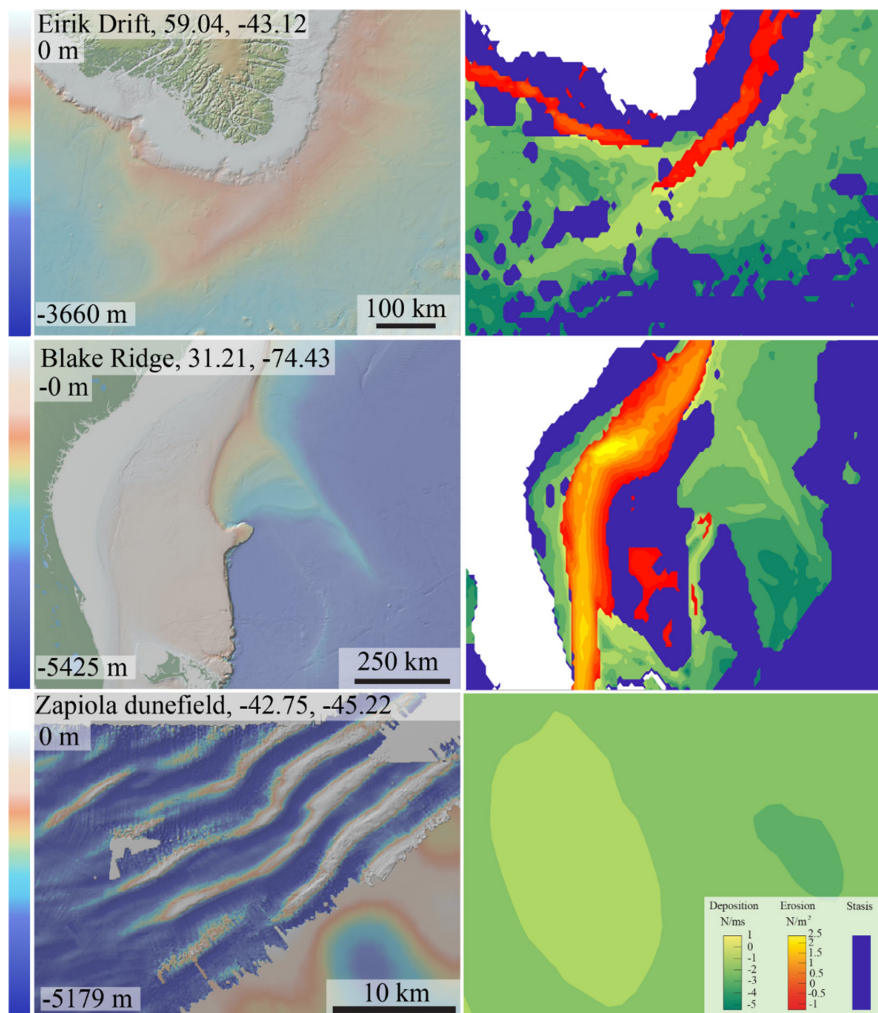


FIGURE 12 Comparison between sonar images of bottom current deposits (left) and the same areas on the prediction (right). Top: The Eirik Moat and Drift System are interpreted to have an erosional moat near the shelf slope break and a depositional drift across the slope and base of the slope (Hunter et al., 2007). These features correspond to erosional and depositional features in the prediction. Middle: The Blake Ridge is a large bottom current-driven sediment accumulation, which is visible on sonar images as a roughly triangular sediment mound. Note that the depositional zone in the sonar image corresponds in planform geometry to the depositional region in the prediction. Bottom: The Zapiola Ridge abyssal wavefield is a large bottom current depositional zone on the abyssal plane offshore Argentina (Volkov & Fu, 2008). This region is shown as a large depositional zone in the prediction. Values in the legend are in logarithmic scale. Scale shown in the Bottom right image is used for all the modelled images shown.

as elongate erosional zones ('moats') surrounded by relatively extensive depositional areas ('drifts', Figures 9 and 16). In contrast to moat and drift systems, plastered drift systems are defined as contourite depositional areas that collect fine-grained sediments from the water column and, where shear stresses are relatively high, deposit ('coat' or, 'plaster') these sediments onto continental slopes. Such areas are visible on the modelled maps as extensive (up to hundreds-of-km long) patches of sediment deposition (Figure 16). Our modelled map predictions also show regions containing extensive abyssal wavefields, which are large depositional regions on the abyssal plain that are largely separated from continental slopes. Such systems are bottom current depositional systems that somewhat

defy the intent of the term 'contourite' as they do not deposit in association with the seafloor contours, but rather form extensive deep marine depositional zones. Abyssal wavefields can contain a wide variety of sediment waves of various morphologies including barchan dunes (Carnegie Ridge; Lonsdale & Spiess, 1977; Lonsdale & Malfait, 1974), transverse mudwaves (e.g. Zapiola drift) or linear dunes (e.g. Feni drift). In contrast to subaerial aeolian systems these 'deserts of the deep' (Beelen, 2021) are comprised of fine-grained muds and clays and are sculpted over extremely long timescales by continuous bottom currents (Lonsdale & Malfait, 1974). Most sediment waves in this setting have been shown to migrate against the dominant current direction (Symons et al., 2016).

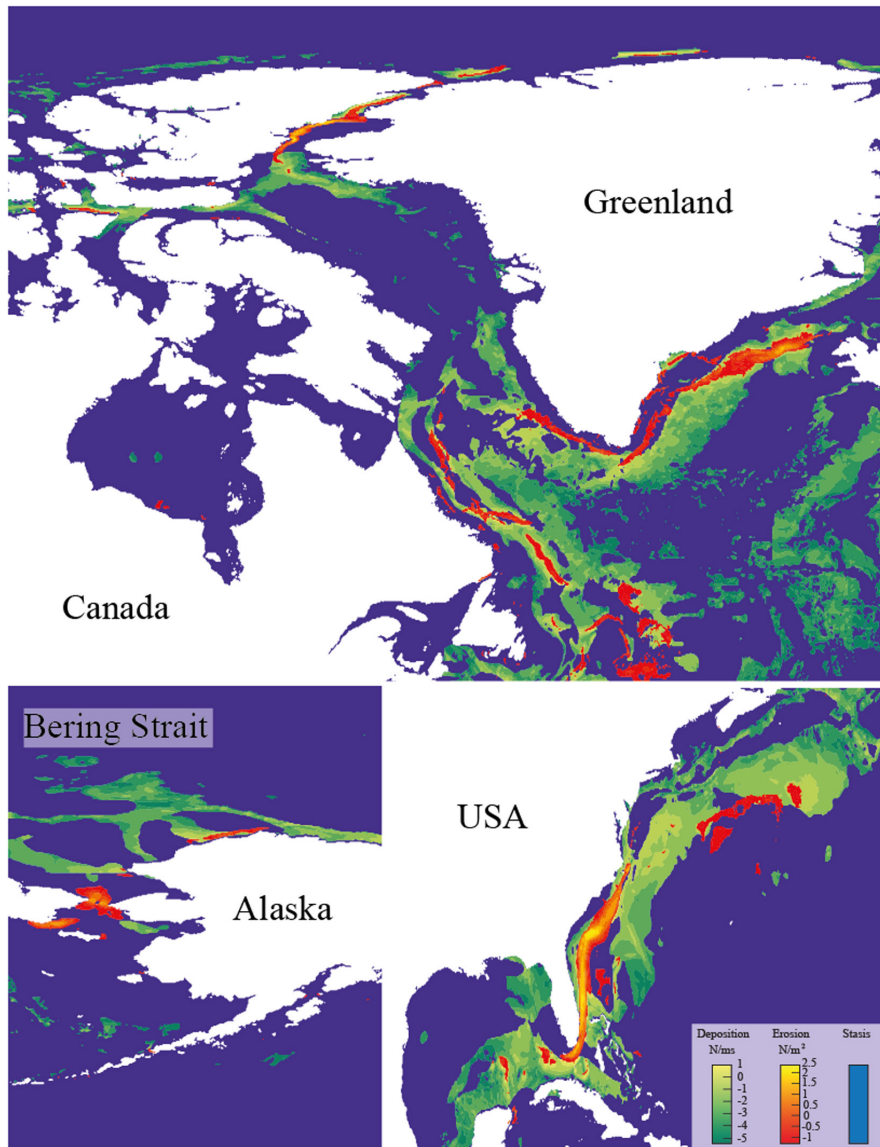


FIGURE 13 Depositional and erosional bottom current systems around North America. (a) Elongate moat (red) and drift (green) systems are formed by the impingement of boundary currents around Greenland. Narrow sea straits between the Nanavut Islands generate erosion. (b) The Bering Strait, between the landmasses of Alaska and Russia, has amplified tidal currents which generate erosion toward the center of the Strait and deposition at the strait's north and south entrances. (c) Intense Gulf Stream Boundary currents occur off the East Coast of the United States and generate extensive zones of erosion at the shelf margin toe of the slope and around the carbonate margins of South Florida. Deposition occurs on the eastern shelf where terrestrial sediments feed the formation of seafloor constructs. Values in the legend are in logarithmic scale.

6.2 | Hemispheric distribution

Based on the outcomes modelled in this study, a marked difference exists in the depositional character of bottom currents found in the northern versus the southern hemisphere of the Earth. As explained in the background section of this paper, both deep ocean sediment supply and bottom shear stress are locally amplified by the obstruction of large landmasses. The northern hemisphere contains about two times more landmass than the southern hemisphere and this invokes a disparity in the distribution of contourites. Furthermore, mechanisms of bottom current deposition are also markedly different between the hemispheres. Models and real-world examples show that the northern hemisphere mainly has deposition on continental slopes and in some regions of the abyssal plain, whereas in the Southern hemisphere, most bottom current deposition and erosion takes place on the

abyssal plain as well as near submarine landmasses like Zealandia and the Kerguelen Plateaus. (Figure 17). As a result, contourite types like plastered drifts and moat and drift systems that frequently occur in proximity to continental shelves are common in the northern hemisphere, but such systems are rare in the southern oceans.

Other regions where bottom current deposition is relatively rare are enclosed basins surrounded by land such as enclosed seas (e.g. the Mediterranean Sea). The importance of such areas should be recognized when examining records of ancient currents as they are typically not connected to the global thermohaline current conveyor system. Unfortunately, a disproportionate number of outcrop-based geological and sedimentological studies are based on foreland basin deposits where thermohaline bottom currents are rare (e.g. Beelen et al., 2021). In some cases, researchers should be cautious when applying interpretations of thermohaline bottom current controlled

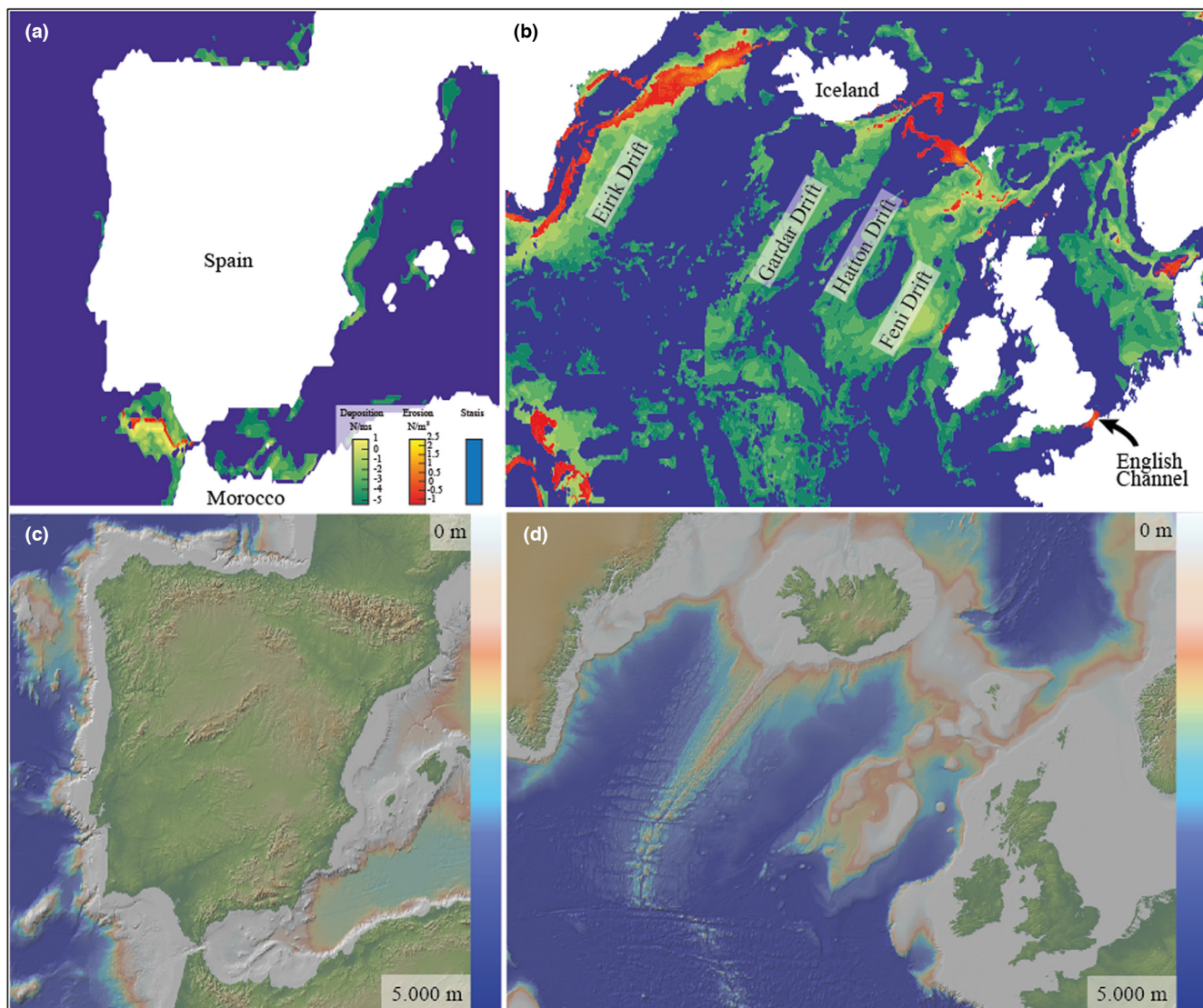


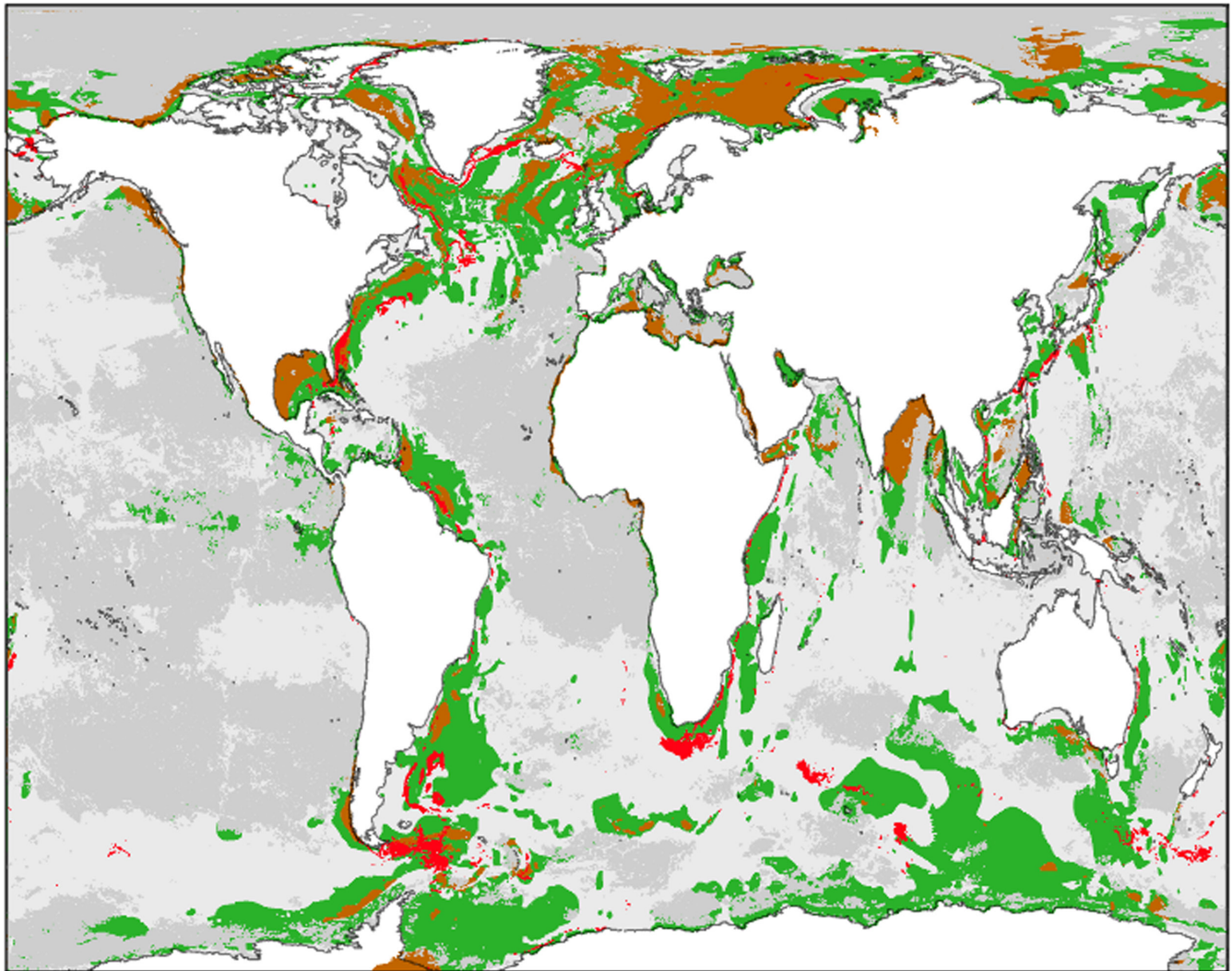
FIGURE 14 Depositional and erosional bottom current systems around Western Europe. (a) contourites are deposited south of Spain where Mediterranean Outflow Water moving between Spain and Morocco erodes and deposits sediments on the seafloor. (b) The North Atlantic is a major zone of bottom current deposition. Several large drifts sit adjacent to one another (i.e. Feni Drift, Gardar Drift). Erosion is occurring between adjacent landmasses (i.e. English Channel) in areas near the base of the continental slope east of Nova Scotia, or across the area of the North Sea between Iceland and the United Kingdom. Legend values are in logarithmic scale.

deposits on rocks that formed in the foreland, hinterland, strike slip or other types of topographically isolated marine basins. In many cases, such areas are not connected to the global thermohaline bottom current conveyors and tend to experience limited shear stress by thermohaline geostrophic currents.

6.3 | Deposition and erosion inferred directly from shear stress

Predicting the depositional or erosional character of currents in many settings has been a historic research pursuit in the field of sedimentology (e.g. Einstein, 1950).

Typically, studies concerned with this topic, infer the sedimentological behaviour of currents by examining critical shear stresses and other factors related to the sediments and hydraulics of a system. In this study, we take a different approach and consider mapped extents of bottom current depositional systems as a primary input to developing a predictive model for contourite systems, while largely ignoring hydraulics and shear stress thresholds like the Shields parameter (Shields, 1936). There are several reasons why we believe that for the purposes of this study, our methodology is more accurate. First, efforts in finding a universal threshold for incipient motion have only been partly successful, and may not be useful across a wide range of real-world settings (e.g. Lavelle & Mofjeld, 1987).



- Bottom current deposition
- Bottom current erosion
- Too much sediment supply (mostly gravitational deposition; turbidites)
- Not enough sediment supply (stasis and some pelagic deposition)
- Not enough bottom shear stress (stasis and some pelagic deposition)

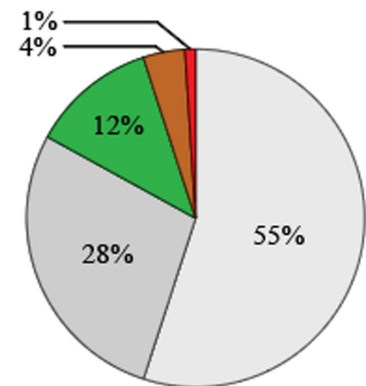


FIGURE 15 Map showing all five regimes demarcated by the four cutoff values. (1) Bottom current deposition (green). (2) Too much bottom shear stress (red). (3) Too much sediment supply (brown). (4) Not enough sediment supply (light grey). (5) Not enough bottom shear stress (dark grey) and each regime is characterized by a sedimentological interpretation. (1) Contourites and abyssal wavefields. (2) Zones of bottom current erosion and possibly the deposition of coarse-grained contourites. (3) Depositional systems dominated by turbidity currents with limited impact of bottom currents. (4) Slow deposition of condensed pelagites. (5) Not enough bottom shear stress and the deposition of pelagites. Pie diagram showing the percentage of the ocean floor covered by bottom current deposition, erosion and various types of bottom current stasis.

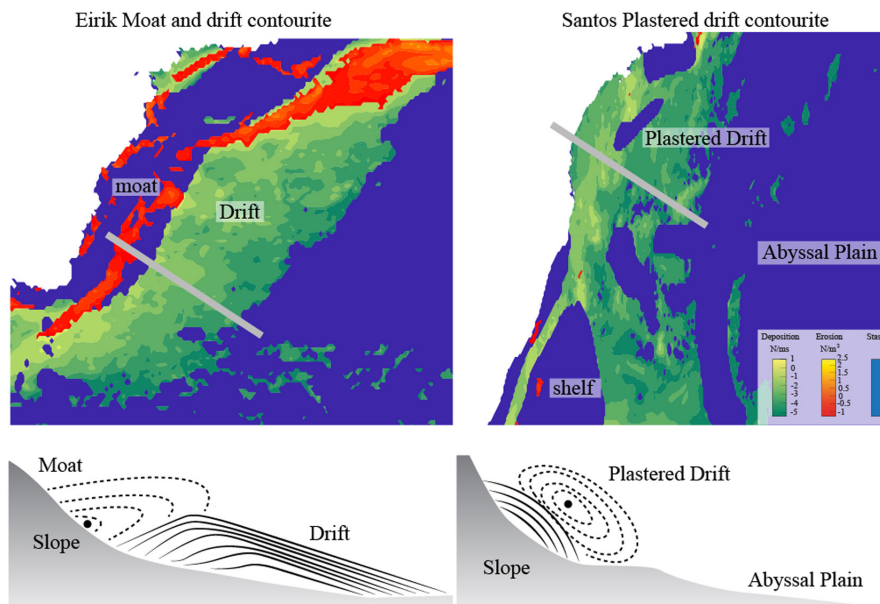
Second, there is very limited information on 'effective' grain sizes at the ocean floor. Fine-grained clayey material that is pervasive in deep water settings, has the

tendency to flocculate, which significantly alters its 'effective' grain size (e.g. Schieber et al., 2013). Since the degree and preservation of flocculation are largely unknown, it

TABLE 4 Regions with common bottom current deposition, erosion and stasis based on our prediction.

Deposition	Erosion	Stasis
Continental slopes	Continental slopes	Mid-oceanic ridges
Barotropic vortices	Sea straits	Regions of vertical water motion like upwelling and bottom current formation
Abyssal regions with significant topography		Partially, or completely enclosed basins like bays and Mediterranean seas
Some continental shelves		Some continental shelves

FIGURE 16 Comparison between model results and schematic, cross-sectional models that represent the plan from geometries. Cross-sectional models are developed from seismic data by Faugères et al. (1999). The figure shows a map view of a moat and drifts deposit, located southeast of Greenland (Eirik drift), and a map view of a plastered drift deposit located off the coast of Uruguay.



is difficult to predict deposition and erosion directly from theory without making use of actual observations. Third, there is limited information on the actual grain size and sediment type distributions on the ocean floor. Sea floor sediment type maps have been published, for example, in Dutkiewicz et al. (2015), but these are suboptimal for use in this study, as they give little direct information on grain sizes. This lack of important data presents substantial uncertainty, pushing us to opt for a model that relies on direct observations of seafloor morphologies. Future work can expand on this study by populating the models presented here with local information on sediment grain sizes when such data become more widely available.

6.4 | Bottom current variability

Thran et al. (2018) present evidence demonstrating that contourite deposition is both correlated to persistent bottom current strength, and also the variability in bottom current intensity. In this study, we use a single model run

that has monthly averaged bottom current strength and, therefore, does not include temporal variabilities. The data from Thran et al. (2018) also show that regions of high variability are strongly spatially aligned with areas of high sustained current intensity. The character of rapid (seasonal or sub-seasonal) bottom current variability is also less well understood than the yearly averaged bottom current intensity and, therefore, cannot be modelled as accurately as year-round averaged sustained intensities. Because of these factors, we believe that including rapid bottom current variability to our prediction is an interesting future research pursuit but is currently not well-enough understood or modelled to use in a prediction such as the one presented in this study.

7 | CONCLUSIONS

This study integrates three types of oceanographic data to predict the distribution of bottom current deposition and erosion. These data types are as follows: (1) models

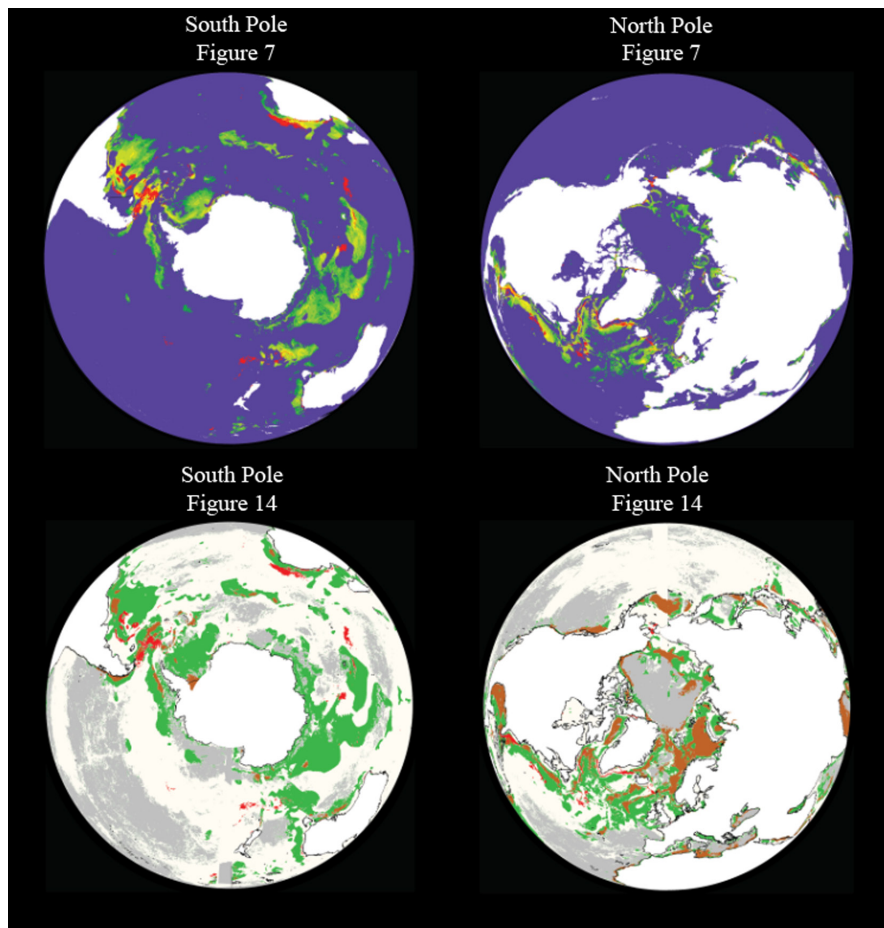


FIGURE 17 Polar projections of the prediction. Left. North Polar project, Eight south polar projection. These projections demonstrate that bottom current deposition and erosion are mostly controlled by the location of the major landmasses in the northern hemisphere, while in the southern ocean, the bottom current activity is mostly controlled by submarine features for example the Kerguelen plateau.

of bottom shear stress from the HYCOM numerical ocean model (Chassignet et al., 2019), (2) sediment thickness from the GlobSed ocean sediment thickness map (Straume et al., 2019) and (3) a map of known contourites and bottom current deposit occurrences (the contourite atlas) by Claus et al. (2017). We use an especially well-mapped area of the Western Atlantic Ocean as a subset of our data to train our model to known occurrences of bottom current deposits. Regimes for likely bottom current deposition and erosion are derived from this model training exercise and these regimes are then used to develop a global prediction. We define three conditions across the ocean floor; bottom current deposition, bottom current erosion and bottom current stasis (neither deposition nor erosion). The planform dispersal of these conditions is then used to formulate generalized patterns that govern the incidence and dispersal of depositional and erosional bottom current systems across the world's oceans. Areas showing high probability for bottom current deposition include continental slopes affected by boundary currents and barotropic vortices, and around submarine mounds, platforms and other obstructions on the seafloor. Areas showing high probability of erosion include confined areas (e.g. sea straits) and continental slopes affected by strong erosional boundary currents. Areas showing a high probability for stasis include

zones of deep water upwelling, zones of deepwater formation, mid-ocean ridges, some continental shelves that have limited bottom shear stress, and enclosed basins and seas.

The results presented here can lead to improved models for seafloor mining, energy extraction and construction of deep ocean infrastructure as well as a more complete understanding of the conditions of thermohaline deposition and erosion on the ocean floor. Future improvements to this study can be made by populating the data presented here with additional information such as ocean floor lithologies, sediment grain sizes and long-term and short-term variations in bottom current velocities.

ACKNOWLEDGEMENTS

We would like to thank the members and research staff of the Sedimentary Analogs Database and Research Consortium (SAnD) for their generous support.

FUNDING STATEMENT

Funding was provided through the SAnD Consortium.


PEER REVIEW

The peer review history for this article is available at <https://www.webofscience.com/api/gateway/wos/peer-review/10.1111/bre.12788>.

DATA AVAILABILITY STATEMENT

All data generated or analysed during this study are included in this published article (and its supplementary information files).

TWITTER

Daan Beelen  @daanosaurus_rex

REFERENCES

- Antrim, C. L. (2005). What was old is new again: Economic potential of deep ocean minerals the second time around. In *Proceedings of OCEANS 2005 MTS/IEEE* (pp. 1311–1318). IEEE.
- Bankole, S., Buckman, J. O., & Stow, D. A. V. (2020). Unusual components within a fine-grained contourite deposit: Significance for interpretation of provenance and the contourite budget. *Minerals*, 2020(10), 488. <https://doi.org/10.3390/min10060488>
- Baringer, M. O. N., & Price, J. F. (1999). A review of the physical oceanography of the Mediterranean outflow. *Marine Geology*, 155(1–2), 63–82. [https://doi.org/10.1016/S0025-3227\(98\)00141-8](https://doi.org/10.1016/S0025-3227(98)00141-8)
- Beelen, D. (2021). *Sedimentology of bottom current processes and their bedforms*. The 2021-Mines Theses & Dissertations.
- Beelen, D., Wood, L. J., Zaghoul, M. N., Arts, M., & Sarg, F. (2021). *Shallow or deep? A reinterpretation of the Rifian Corridor's unique sandy contourites*. EarthArXiv.
- Bonaldo, D., Benetazzo, A., Bergamasco, A., Campiani, E., Fogliani, F., Sclavo, M., Trincardi, F., & Carniel, S. (2016). Interactions among Adriatic continental margin morphology, deep circulation and bedform patterns. *Marine Geology*, 375, 82–98.
- Breitzke, M., Wiles, E., Krockner, R., Watkeys, M. K., & Jokat, W. (2017). Seafloor morphology in the Mozambique Channel: Evidence for long-term persistent bottom-current flow and deep-reaching eddy activity. *Marine Geophysical Research*, 38(3), 241–269.
- Bullister, J. L., Rhein, M., & Mauritzen, C. (2013). Deepwater formation. In *International geophysics* (Vol. 103, pp. 227–253). Academic Press.
- Chassignet, E. P., Hurlburt, H. E., Metzger, E. J., Smedstad, O. M., Cummings, J. A., Halliwell, G. R., Bleck, R., Baraille, R., Wallcraft, A. J., Lozano, C., Tolman, H. L., Srinivasan, A., Hankin, S., Cornillon, P., Weisberg, R., Barth, A., He, R., Werner, F., & Wilkin, J. (2009). US GODAE: Global ocean prediction with the HYbrid Coordinate Ocean Model (HYCOM). *Oceanography*, 22(2), 64–75. <https://doi.org/10.5670/oceanog.2009.39>
- Chelton, D. B., & Schlax, M. G. (1996). Global observations of oceanic Rossby waves. *Science*, 272(5259), 234–238.
- Chen, H., Zhang, W., Xie, X., & Ren, J. (2019). Sediment dynamics driven by contour currents and mesoscale eddies along continental slope: A case study of the northern South China Sea. *Marine Geology*, 409, 48–66.
- Cheng, L., Trenberth, K. E., Gruber, N., Abraham, J. P., Fasullo, J. T., Li, G., Mann, M. E., Zhao, X., & Zhu, J. (2020). Improved estimates of changes in upper ocean salinity and the hydrological cycle. *Journal of Climate*, 33(23), 10357–10381.
- Claus, S., De Hauwere, N., Vanhoorne, B., Deckers, P., Souza Dias, F., Hernandez, F., & Mees, J. (2014). Marine regions: Towards a global standard for georeferenced marine names and boundaries. *Marine Geodesy*, 37(2), 99–125.
- Claus, S., De Hauwere, N., Vanhoorne, B., Hernandez, F., & Mees, J. (2017). MarineRegions.org [WWW document]. MarineRegions.org
- Davis, R. A., Jr., & Dalrymple, R. W. (Eds.). (2011). *Principles of tidal sedimentology*. Springer Science and Business Media.
- Dutkiewicz, A., Müller, R. D., O'Callaghan, S., & Jónasson, H. (2015). Census of seafloor sediments in the world's ocean. *Geology*, 43(9), 795–798.
- Einstein, H. A. (1950). *The bed-load function for sediment transportation in open channel flows* (No. 1026). US Department of Agriculture.
- Ercilla, G., Juan, C., Hernández-Molina, F. J., Bruno, M., Estrada, F., Alonso, B., Casas, D., Farran, M., Llave, E., García, M., Vázquez, J. T., D'Acremont, E., Gorini, C., Palomino, D., Valencia, J., El Moumni, B., & Ammar, A. (2016). Significance of bottom currents in deep-sea morphodynamics: An example from the Alboran Sea. *Marine Geology*, 378, 157–170.
- Fabbi, S., Citton, P., Romano, M., & Cipriani, A. (2016). Detrital events within pelagic deposits of the Umbria-Marche Basin (northern Apennines, Italy): Further evidence of early cretaceous tectonics. *Journal of Mediterranean Earth Sciences*, 8, 39–52.
- Faugères, J. C., Mézerais, M. L., & Stow, D. A. (1993). Contourite drift types and their distribution in the north and South Atlantic Ocean basins. *Sedimentary Geology*, 82(1–4), 189–203.
- Faugères, J. C., & Mulder, T. (2011). Contour currents and contourite drifts. In *Developments in sedimentology* (Vol. 63, pp. 149–214). Elsevier.
- Faugères, J. C., Stow, D. A., Imbert, P., & Viana, A. (1999). Seismic features diagnostic of contourite drifts. *Marine Geology*, 162(1), 1–38.
- Flood, R. D. (1981). Distribution, morphology, and origin of sedimentary furrows in cohesive sediments, Southampton Water. *Sedimentology*, 28(4), 511–529.
- Flood, R. D., Hollister, C. D., & Lonsdale, P. (1979). Disruption of the Feni sediment drift by debris flows from Rockall Bank. *Marine Geology*, 32(3–4), 311–334.
- Flood, R. D., Shor, A. N., & Manley, P. L. (1993). Morphology of abyssal mudwaves at project MUDWAVES sites in the Argentine basin. *Deep Sea Research Part II: Topical Studies in Oceanography*, 40(4–5), 859–888.
- Fonnesu, M., Palermo, D., Galbiati, M., Marchesini, M., Bonamini, E., & Bendias, D. (2020). A new world-class deep-water play-type, deposited by the syndepositional interaction of turbidity flows and bottom currents: The giant Eocene coral field in northern Mozambique. *Marine and Petroleum Geology*, 111, 179–201.
- Garrett, C., & Munk, W. (1979). Internal waves in the ocean. *Annual Review of Fluid Mechanics*, 11(1), 339–369.
- Gong, C., Wang, Y., Xu, S., Pickering, K. T., Peng, X., Li, W., & Yan, Q. (2015). The northeastern South China Sea margin created by the combined action of down-slope and along-slope processes: Processes, products and implications for exploration and paleoceanography. *Marine and Petroleum Geology*, 64, 233–249.
- Gonthier, E. G., Faugères, J. C., & Stow, D. A. V. (1984). Contourite facies of the Faro drift, gulf of Cadiz. *Geological Society, London, Special Publications*, 15(1), 275–292.
- Grant, W. D., & Madsen, O. S. (1986). The continental-shelf bottom boundary layer. *Annual review of fluid mechanics*, 18(1), 265–305.

- Haupt, B. J., Schäfer-Neth, C., & Statterger, K. (1994). Modeling sediment drifts: A coupled oceanic circulation-sedimentation model of the northern North Atlantic. *Paleoceanography*, 9(6), 897–916.
- Heezen, B. C. (1959). Dynamic processes of abyssal sedimentation: Erosion, transportation, and redeposition on the deep-sea floor. *Geophysical Journal International*, 2(2), 142–163.
- Heezen, B. C., & Hollister, C. D. (1972). Face of the deep.
- Hernández-Molina, F. J., Maldonado, A., & Stow, D. A. V. (2008). Abyssal plain contourites. *Developments in Sedimentology*, 60, 345–378.
- Hernández-Molina, F. J., Paterlini, M., Violante, R., Marshall, P., de Isasi, M., Somoza, L., & Rebesco, M. (2009). Contourite depositional system on the argentine slope: An exceptional record of the influence of Antarctic water masses. *Geology*, 37(6), 507–510.
- Hernández-Molina, F. J., Sierro, F. J., Llave, E., Roque, C., Stow, D. A. V., Williams, T., Lofi, J., Van der Schee, M., Arnáiz, A., Ledesma, S., Rosales, C., Rodríguez-Tovar, F. J., Pardo-Igúzquiza, E., & Brackenridge, R. E. (2016). Evolution of the gulf of Cadiz margin and Southwest Portugal contourite depositional system: Tectonic, sedimentary and paleoceanographic implications from IODP expedition 339. *Marine Geology*, 377, 7–39.
- Hollister, C. D., & Heezen, B. C. (1972). Geologic effects of ocean bottom currents: Western North Atlantic. *Marine Geology*, 39, 277–310.
- Hüneke, H., Hernández-Molina, F. J., Rodríguez-Tovar, F. J., Llave, E., Chiarella, D., Mena, A., & Stow, D. A. (2021). Diagnostic criteria using microfacies for calcareous contourites, turbidites and pelagites in the Eocene–Miocene slope succession, southern Cyprus. *Sedimentology*, 68(2), 557–592.
- Hüneke, H., & Stow, D. A. V. (2008). Identification of ancient contourites: Problems and palaeoceanographic significance. *Developments in Sedimentology*, 60, 323–344.
- Hunter, S., Wilkinson, D., Louarn, E., McCave, I. N., Rohling, E., Stow, D. A., & Bacon, S. (2007). Deep western boundary current dynamics and associated sedimentation on the Eirik drift, southern Greenland margin. *Deep Sea Research Part I: Oceanographic Research Papers*, 54(12), 2036–2066.
- IHI Corporation. (2019). IHI Demonstrated the World's Largest Ocean Current Turbine for the First Time in the World. <https://www.ihico.jp/en>
- Jacox, M. G., Edwards, C. A., Hazen, E. L., & Bograd, S. J. (2018). Coastal upwelling revisited: Ekman, Bakun, and improved upwelling indices for the US west coast. *Journal of Geophysical Research: Oceans*, 123(10), 7332–7350.
- Kapoor, D. C. (1981). General bathymetric chart of the oceans (GEBCO). *Marine Geodesy*, 5(1), 73–80.
- Knutz, P. C. (2008). Palaeoceanographic significance of contourite drifts. *Developments in Sedimentology*, 60, 511–535.
- Lavelle, J. W., & Mofjeld, H. O. (1987). Do critical stresses for incipient motion and erosion really exist? *Journal of Hydraulic Engineering*, 113(3), 370–385.
- Llave, E., Hernández-Molina, F. J., Somoza, L., Stow, D. A. V., & Del Río, V. D. (2007). Quaternary evolution of the contourite depositional system in the Gulf of Cadiz. *Geological Society, London, Special Publications*, 276(1), 49–79.
- Lonsdale, P., & Malfait, B. (1974). Abyssal dunes of foraminiferal sand on the Carnegie ridge. *Geological Society of America Bulletin*, 85(11), 1697–1712.
- Lonsdale, P., & Spiess, F. N. (1977). Abyssal bedforms explored with a deeply towed instrument package. In *Developments in sedimentology* (Vol. 23, pp. 57–75). Elsevier.
- McCave, I. N., & Tucholke, B. E. (1986). Deep current-controlled sedimentation in the western North Atlantic. In P. R. Vogt & B. E. Tucholke (Eds.), *DNAG, Geology of North America The Western North Atlantic Region*. GeoScienceWorld.
- Miramontes, E., Eggenhuisen, J. T., Jacinto, R. S., Poneti, G., Pohl, F., Normandeau, A., & Hernández-Molina, F. J. (2020). Channel-levee evolution in combined contour current–turbidity current flows from flume-tank experiments. *Geology*, 48(4), 353–357.
- Mulder, T., Faugères, J. C., & Gonthier, E. (2008). Mixed turbidite–contourite systems. *Developments in sedimentology*, 60, 435–456. [https://doi.org/10.1016/S0070-4571\(08\)10021-8](https://doi.org/10.1016/S0070-4571(08)10021-8)
- Mulder, T., Syvitski, J. P., Migeon, S., Faugères, J. C., & Savoye, B. (2003). Marine hyperpycnal flows: Initiation, behavior and related deposits. A review. *Marine and Petroleum Geology*, 20(6–8), 861–882. <https://doi.org/10.1016/j.marpetgeo.2003.09.001>
- Müller, R. D., Sdrolias, M., Gaina, C., & Roest, W. R. (2008). Age, spreading rates, and spreading asymmetry of the world's ocean crust. *Geochemistry, Geophysics, Geosystems*, 9(4), 1–19.
- Pellegrini, C., Maselli, V., & Trincardi, F. (2016). Pliocene–quaternary contourite depositional system along the south-western Adriatic margin: Changes in sedimentary stacking pattern and associated bottom currents. *Geo-Marine Letters*, 36(1), 67–79.
- Peukert, A., Schoening, T., Alevizos, E., Köser, K., Kwasnitschka, T., & Greinert, J. (2018). Understanding Mn-nodule distribution and evaluation of related deep-sea mining impacts using AUV-based hydroacoustic and optical data. *Biogeosciences*, 15(8), 2525–2549.
- Rebesco, M., Camerlenghi, A., & Van Loon, A. J. (2008). Contourite research: A field in full development. *Developments in Sedimentology*, 60, 1–10.
- Rebesco, M., Hernández-Molina, F. J., Van Rooij, D., & Wåhlin, A. (2014). Contourites and associated sediments controlled by deep-water circulation processes: State-of-the-art and future considerations. *Marine Geology*, 352, 111–154.
- Rebesco, M., & Stow, D. (2001). Seismic expression of contourites and related deposits: A preface. *Marine Geophysical Researches*, 22(5), 303–308.
- Sánchez-García, L., de Andrés, J. R., Martín-Rubí, J. A., & Louchouart, P. (2009). Diagenetic state and source characterization of marine sediments from the inner continental shelf of the Gulf of Cádiz (SW Spain), constrained by terrigenous biomarkers. *Organic Geochemistry*, 40(2), 184–194.
- Savoye, B., Babonneau, N., Dennielou, B., & Bez, M. (2009). Geological overview of the Angola–Congo margin, The Congo deep-sea fan and its submarine valleys. *Deep Sea Research Part II: Topical Studies in Oceanography*, 56(23), 2169–2182.
- Schieber, J., Southard, J. B., Kissling, P., Rossman, B., & Ginsburg, R. (2013). Experimental deposition of carbonate mud from moving suspensions: Importance of flocculation and implications for modern and ancient carbonate mud deposition. *Journal of Sedimentary Research*, 83(11), 1026–1032.
- Shanmugam, G. (2017). Contourites: Physical oceanography, process sedimentology, and petroleum geology. *Petroleum Exploration and Development*, 44(2), 183–216.
- Shields, A. (1936). *Anwendung der Aehnlichkeitsmechanik und der Turbulenzforschung auf die Geschiebepbewegung*. PhD Thesis. Technical University Berlin.

- Slotman, A., & Cartigny, M. J. (2020). Cyclic steps: Review and aggradation-based classification. *Earth-Science Reviews*, 201, 102949.
- Spall, M. A. (1996). Dynamics of the Gulf stream/deep western boundary current crossover. Part II: Low-frequency internal oscillations. *Journal of Physical Oceanography*, 26(10), 2169–2182.
- Stewart, H. A., & Long, D. (2012). The timing and significance of gully incision on the eastern flank of the Faroe–Shetland Channel and its impact on seafloor infrastructure. *Near Surface Geophysics*, 10(4), 317–331.
- Stow, D., Smillie, Z., & Esentia, I. P. (2018). Deep-sea bottom currents: Their nature and distribution. In *Encyclopedia of ocean sciences: earth systems and environmental sciences*. Springer.
- Stow, D. A., Faugères, J. C., Viana, A., & Gonthier, E. (1998). Fossil contourites: A critical review. *Sedimentary Geology*, 115(1–4), 3–31.
- Stow, D. A., Hernández-Molina, F. J., Llave, E., Sayago-Gil, M., Díaz del Río, V., & Branson, A. (2009). Bedform-velocity matrix: The estimation of bottom current velocity from bedform observations. *Geology*, 37(4), 327–330.
- Stow, D. A. V., Hunter, S., Wilkinson, D., & Hernández-Molina, F. J. (2008). The nature of contourite deposition. In M. Rebesco & A. Camerlenghi (Eds.), *Contourites, Developments in Sedimentology Series* (Vol. 60, pp. 143–157). Elsevier.
- Stow, D. A. V., & Lovell, J. P. B. (1979). Contourites: Their recognition in modern and ancient sediments. *Earth-Science Reviews*, 14(3), 251–291.
- Straume, E. O., Gaina, C., Medvedev, S., Hochmuth, K., Gohl, K., Whittaker, J. M., Doornenbal, J. C., & Hopper, J. R. (2019). GlobSed: Updated total sediment thickness in the world's oceans. *Geochemistry, Geophysics, Geosystems*, 20(4), 1756–1772.
- Symons, W. O., Sumner, E. J., Talling, P. J., Cartigny, M. J., & Clare, M. A. (2016). Large-scale sediment waves and scours on the modern seafloor and their implications for the prevalence of supercritical flows. *Marine Geology*, 371, 130–148.
- Thran, A. C., Dutkiewicz, A., Spence, P., & Müller, R. D. (2018). Controls on the global distribution of contourite drifts: Insights from an eddy-resolving ocean model. *Earth and Planetary Science Letters*, 489, 228–240. <https://doi.org/10.1016/j.epsl.2018.02.044>
- Toucanne, S., Mulder, T., Schönfeld, J., Hanquiez, V., Gonthier, E., Duprat, J., Cremer, M., & Zaragosi, S. (2007). Contourites of the Gulf of Cadiz: A high-resolution record of the paleocirculation of the Mediterranean outflow water during the last 50,000 years. *Palaeogeography, Palaeoclimatology, Palaeoecology*, 246(2–4), 354–366.
- Trossman, D. S., Arbic, B. K., Garner, S. T., Goff, J. A., Jayne, S. R., Metzger, E. J., & Wallcraft, A. J. (2013). Impact of parameterized lee wave drag on the energy budget of an eddying global ocean model. *Ocean Modelling*, 72, 119–142.
- Trossman, D. S., Arbic, B. K., Richman, J. G., Garner, S. T., Jayne, S. R., & Wallcraft, A. J. (2016). Impact of topographic internal lee wave drag on an eddying global ocean model. *Ocean Modelling*, 97, 109–128.
- Velde, B. (Ed.). (2013). *Origin and mineralogy of clays: Clays and the environment*. Springer Science & Business Media.
- Volkov, D. L., & Fu, L. L. (2008). The role of vorticity fluxes in the dynamics of the Zapiola anticyclone. *Journal of Geophysical Research: Oceans*, 113(C11), 35.20.
- Weaver, P. P. E., & Kuijpers, A. (1983). Climatic control of turbidite deposition on the Madeira abyssal plain. *Nature*, 306(5941), 360–363.
- Xie, L., & Hsieh, W. W. (1995). The global distribution of wind-induced upwelling. *Fisheries Oceanography*, 4(1), 52–67.
- Zenk, W. (2008). Temperature fluctuations and current shear in Antarctic bottom water at the Vema sill. *Progress in Oceanography*, 77(4), 276–284.
- Zhang, G., Qu, H., Chen, G., Zhao, C., Zhang, F., Yang, H., Zhao, Z., & Ma, M. (2019). Giant discoveries of oil and gas fields in global deepwaters in the past 40 years and the prospect of exploration. *Journal of Natural Gas Geoscience*, 4(1), 1–28.

SUPPORTING INFORMATION

Additional supporting information can be found online in the Supporting Information section at the end of this article.

How to cite this article: Beelen, D., & Wood, L. J. (2023). Predicting bottom current deposition and erosion on the ocean floor. *Basin Research*, 35, 1985–2009. <https://doi.org/10.1111/bre.12788>